Extreme Precipitation Analysis at Hinkley Point – Final Report

For - EDF
Date – 20th August 2010
Authors – Thomas Francis, Michael Sanderson, James Dent and Mathew Perry

Prepared by: Thomas Francis (Scientific Consultant)

Michael Sanderson (Senior Scientific Consultant)

Reviewed by: Malcolm Lee (Manager, Scientific Consultancy)

Authorised for issue by: Malcolm Lee (Manager, Scientific Consultancy)

Contents

Executive Summary

- 1 in 100, 1,000 and 10,000 year rainfall amounts for winter and summer have been estimated for Hinkley Point using a combination of observed and modelled rainfall amounts. The 10,000 year estimates fall within the range of Probable Maximum Precipitation (PMP) at Hinkley Point, produced using three different methods (these do not account for climate change) demonstrating that the precipitation amounts are reasonable. The results are summarised in the tables below;

Return Period (years)	Storm Duration	Baseline rainfall estimates (mm)	Winter estimates adj. for climate change (mm)	Summer estimates adj. for climate change (mm)
10,000	15 minutes	145.1	143.1 – 176.8	119.6 – 169.2
	1 hour	163.7	161.2 – 204.0	131.3 – 194.4
	1 day	228.8	223.9 – 307.5	165.5 – 288.7
1,000	15 minutes	69.5	69.2-80.7	60.7-77.8
	1 hour	85.5	85.0-102.5	72.3-98.0
	1 day	145.6	144.2-194.8	107.2-182.0
100	15 minutes	33.3	33.3-37.2	30.4-36.0
	1 hour	44.6	44.7-51.6	39.3-49.5
	1 day	92.6	92.8-122.7	69.8-113.5

Storm Duration	Range of PMP estimates (mm)
15 minutes	104 – 154
1 hour	185 – 210
1 day	285 – 310

- Modelled daily precipitation amounts from the 11 member regional climate model ensemble, which were released alongside the UKCP09 climate projections, have been analysed.

- All estimates of extreme precipitation amounts were calculated using extreme value analysis. Three different approaches were tried. The first, which effectively assumed a uniform increase in extreme precipitation with time, produced only a small increase, whereas the second, where the shape of the extreme precipitation curve was allowed to change, produced much larger precipitation changes. Winter and summer rainfall amounts were not separated. Agreement between individual regional climate model members was poor. Natural variability in and between each member was found to be large causing uncertainty in the extreme value curves to be large. In the third approach efforts were made to

reduce this uncertainty to an acceptable level; a method known as 'bootstrapping' was employed. The resulting distributions were improved, and climate change factors were calculated, this time for summer and winter.

- All members bar one projected an increase in extreme rainfall in winter, whereas changes in extreme summer rainfall are much less certain.

- The climate change factors calculated using the third approach were applied to the baseline 100, 1,000 and 10,000 year rainfall amounts for Hinkley Point estimated using the Flood Estimation Handbook.

- There remains a large spread in the projected extreme precipitation amounts in the 11 member model ensemble, and so these results should be used with caution.

- The ensemble has been generated using the latest science available for extreme value analysis, but some of this science is still being developed and evaluated.

1. Introduction

The Met Office has been requested by EDF to examine the impact of climate change on precipitation extremes (referred to throughout this report as 1 in 100, 1,000 and 10,000 year rainfall) at the proposed site of a new nuclear power station at Hinkley Point in Somerset. This report is the final report and concludes the main findings of the project, summarising the results of estimation of daily and sub-daily precipitation accounting for climate change.

The study at Hinkley Point has been separated into two main phases:

1) Calculating the current estimates of daily and sub-daily extreme precipitation for the 1 in 100, 1,000 and 10,000 year return period and assessing the ability of the Regional Climate Model to modify these estimates, and
2) Prediction of daily and sub-daily estimates accounting for climate change and verification of these outputs using a study of Probable Maximum Precipitation.

This report is split into seven main sections. Following an overview of Hinkley Point, Section 2 details the methodology used to derive the current day or baseline extreme rainfall estimates, which take no account of climate change. Section 3 is dedicated to assessing the feasibility of using the Regional Climate Model (RCM) to modify the baseline estimates to account for climate change. Section 4 explains the methodology used to derive the changes in daily 100, 1,000 and 10,000 year rainfall for seven 30 year periods up to 2099. Section 5 applies these changes to the baseline daily and sub-daily extreme rainfall estimates for Hinkley Point, the results of which are presented in Table 13, and Table 24 and Table 26 in the Appendix. These tables provide a range of estimates for the 100, 1,000 and 10,000 year rainfalls from which a design rainfall depth can be selected for drainage design at Hinkley Point. Section 6 presents a range of estimates of Probable Maximum Precipitation (PMP) at Hinkley Point and Section 7 concludes the final results of the study and provides recommendations and limitations in application of the results.

1.1 Hinkley Point Power Station

Hinkley Point Power Station is situated on the north-facing Somerset coast (Figure 1**)**, approximately 18 km south-west of Weston-Super-Mare and 23 km east of Minehead and 13 km north-west of Bridgewater. The southern coastline of Wales lies little more than 20 km to the north at its nearest point, with the city of Cardiff some 30 km to the north-north-east. Inland from Hinkley Point lies a contrasting variety of topography. The land within 5 km is mostly a mixture of shallow valleys and low hills not exceeding 100 metres. Beyond, to the south-west, the land rises towards the 300-400 metre summit of the Quantock Hills – some 10 km away. Further to the west and south-west lie the extensive uplands of Exmoor reaching a maximum height of 519 metres at Dunkery Beacon. Within a few kilometres to the north-east, east and south-east lie the Somerset Levels – a 20-25 km-wide expanse of mostly very flat, low-lying and damp lands, containing isolated hills and ridges and bounded to the east by the Mendip Hills.

Figure 1. Map of Hinkley Point Power Station and local rain gauges used in this study

2. Daily and sub-daily estimates of extreme precipitation at Hinkley Point for the current climate

2.1 Methodology and data availability

To understand how extreme precipitation may change in the future at Hinkley Point as a result of climate change, the current baseline statistics of maximum rainfalls must be established at this site. The standard practice in assessing current meteorological conditions, at any location, is to use historic records representative of the point of interest to calculate extreme value statistics. The extensive nature of flood research in the UK has resulted in the production of the Flood Estimation Handbook (FEH). This is the source of estimates of storm event and design rainfalls used by The Department for Environment, Food and Rural Affairs, the Environment Agency and drainage designers. The methods have been derived from studying extensive historic records and analyses of rainfall event structures. More information regarding the FEH and methods used to obtain rainfall estimates at a point can be found in the Appendix, Section 9.1. The approach adopted in this study to examine baseline conditions uses the FEH method and then uses standard statistical techniques and local rainfall records to validate the results produced to improve confidence.

2.2 Rain gauge data

In order to check the FEH estimates using individual station records an initial search was undertaken to identify the number of rain gauge records in the vicinity of Hinkley Point. To obtain data most representative of the typical storm events experienced at the site only stations within a 10km radius of the site (321000E, 146000N) and at or below 50 m above ordnance datum (AOD) were included. This initial search produced 11 rain gauge stations in the Met Office digitised database with daily data, with record lengths ranging from between 1 to 50 years. The search also indicated an additional long period of rainfall records held in Met Office archives in paper for Cannington Farm Institute and Brymore House prior to the period of the digitised data.

Three stations were chosen for initial analysis; Cannington Farm Institute, Brymore School and Whitewick Farm, the details of which are presented in Table 1 and locations in relation to Hinkley Point shown in Figure 1. The selection was based on a balance of

achieving the longest possible historical records from sites as near to Hinkley Point as possible.

Gauge ID	Name	Distance from Hinkley Point (km)	Record Length (years)	Easting	Northing	Altitude (AOD)
398383	Whitewick Farm	2.79	45	323600	145300	3
404580	Brymore School	7.43	51	324470	139430	25
404585	Cannington	7.64	45	325535	139852	25

Table 1 - Summary of rain gauge records used in analysis

An initial inspection of the data found some missing months and years in the digitised records at each station and this information is summarised in the Appendix, Section 9.2, Table 21, Table 22 and Table 23. Where a year was found to have 3 or more months of missing data it was excluded from the analysis in an attempt to ensure that rainfall records were unbiased by seasonal effects. The close proximity of the stations to each other suggests that gaps in the Cannington record could be filled by the records from Brymore House and Brymore School. In order to confirm this assumption, a double mass plot of the data recorded simultaneously at each site (1962-1983) is shown in Figure 2.

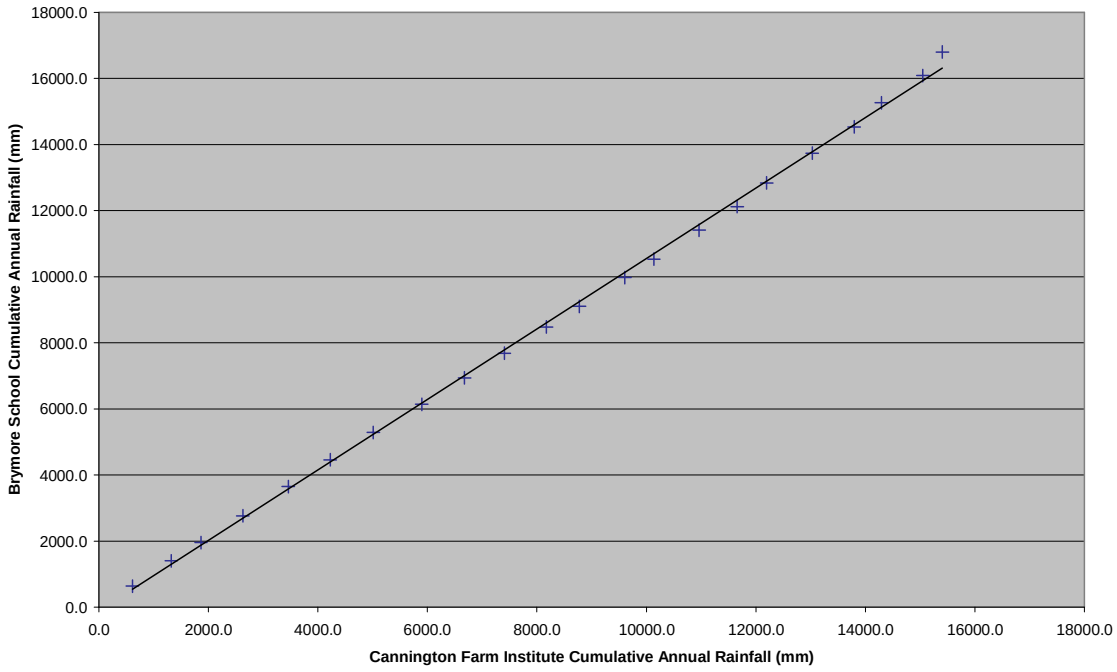

Figure 2. Double mass plot of cumulative annual rainfall at Brymore School and Cannington Farm Institute for 1962-1983

A double mass plot is the standard practice for the assessment of rainfall and river flow records. Any significant deviation from the straight line plotted through the points in Figure 2 would have suggested an inconsistency in one or other of the records.

The records from Brymore School, being the shorter record, have been used to fill the gaps data in the Cannington data set, which along with the data from Brymore House results in an unusually long time series of daily rainfall of 104 years (1905-2009 (record for 1907 missing)). The resultant annual maxima (AMAX) series for Cannington/Brymore is shown in Figure 3. Figure 4 illustrates the AMAX time series compiled for Whitewick Farm for a total of 41 years.

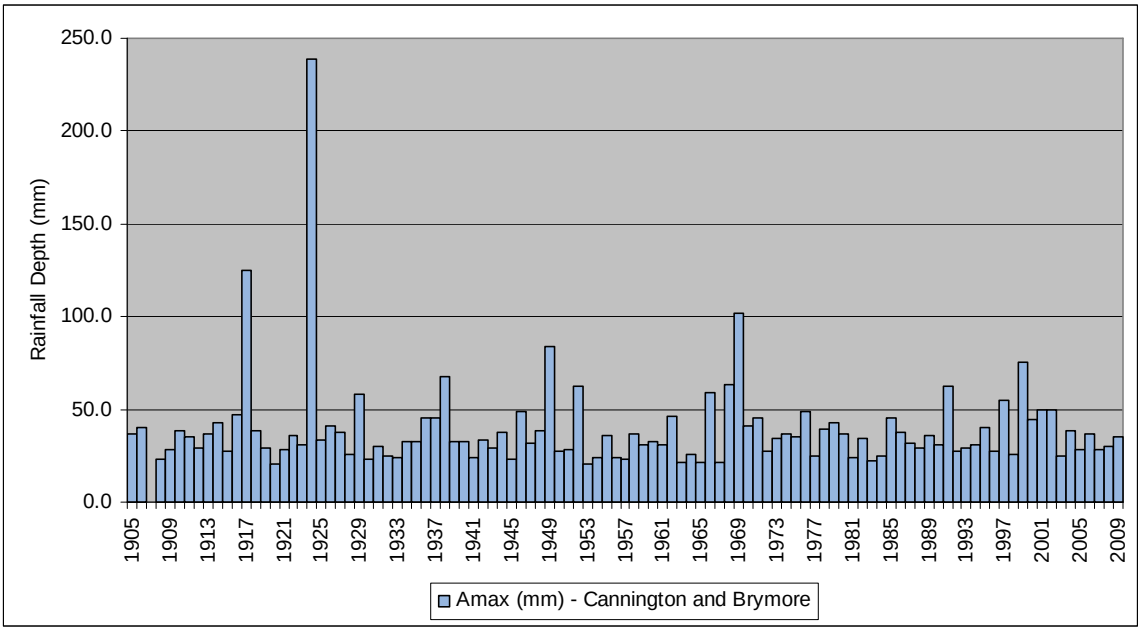

Figure 3. AMAX time series for Cannington/Brymore 1905 - 2009

Figure 3 provides a particularly long record of maximum rainfalls for analysis. The bulk of AMAX records fall between 20.0 and 50.0 mm with a median of 33.4 mm. The peak falls in 1917[1], 1924 and 1969 are particularly prominent with rainfall depth totals of 124.7, 238.8 and 101.6 mm respectively. Whilst the presence of such large events in the record are likely to improve the statistical analysis and extrapolation of the data to provide more confident extreme estimates they may also serve to skew the distribution of the data. The Whitewick Farm record in Figure 4 is more representative of a typical long rainfall record available for analysis in the UK. These shorter records are less likely to include

[1] Rainfall recorded as part of the major 'Bruton' storm, one of the top 5 extreme rainfall events in the English storm record.

very rare extreme events and this is demonstrated by the comparing Figure 3 and Figure 4. The most prominent maximum falls at Whitewick Farm occurred in 1968 and 1969 with rainfall totals of 78.0 and 97.0 mm respectively. The median rainfall depth of the record is very similar to the Cannington/Brymore record at 32.0 mm which suggests that despite the shorter record the distribution of the data is similar to the longer record.

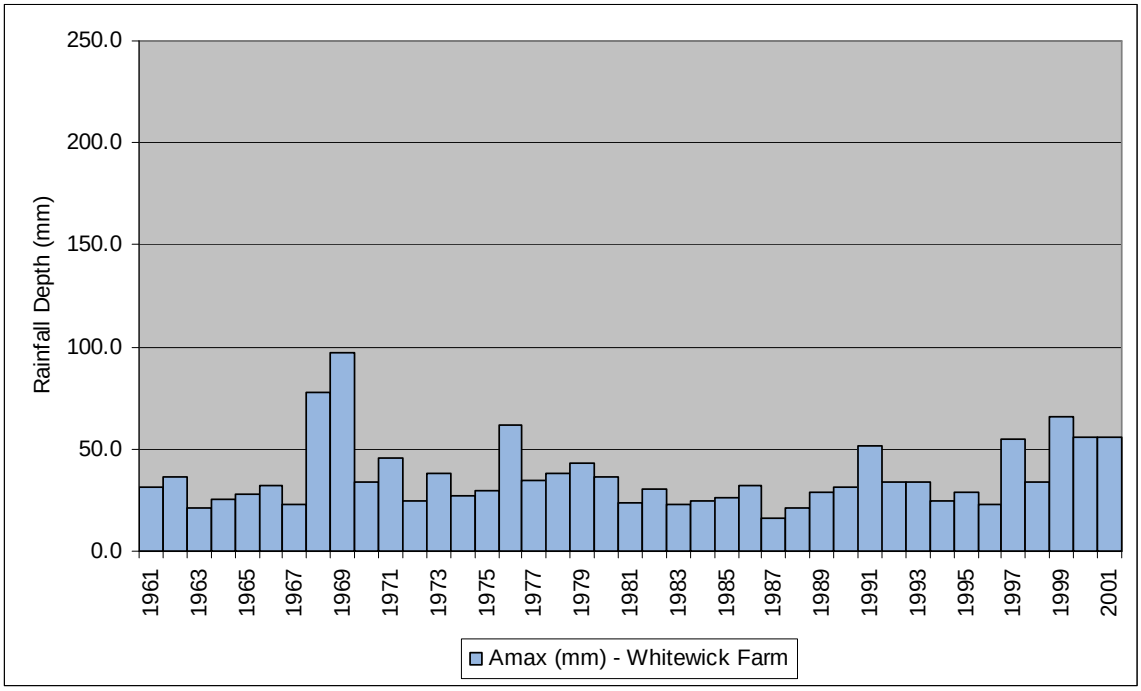

Figure 4. AMAX time series for Whitewick Farm 1961 - 2001

The event which occurred on 18-19 August, 1924, can be placed in the 10 most severe rainfall events anywhere in the UK since 1900. The storm total has been estimated as having a return period of between 13,000 and 14,000 years, and the recorded rainfall of 238.8mm exceeds the FSR estimate of probable maximum precipitation (PMP) for that locality and duration, which is 218mm (Stewart et al., 2010). The event is fully reported in a paper in British Rainfall 1924 (Glasspoole, 1924) and Figure 5 below presents as indication of the extent of the storm which would have also impacted Hinkley Point. This event and the estimates made in the Reservoir Safety Project (Stewart et al., 2010) provide good evidence of the risk that Hinkley Point could be subjected to rare extreme events in the future and as a reference to check against estimates of extreme rainfall made in the different analyses throughout the rest of the study.

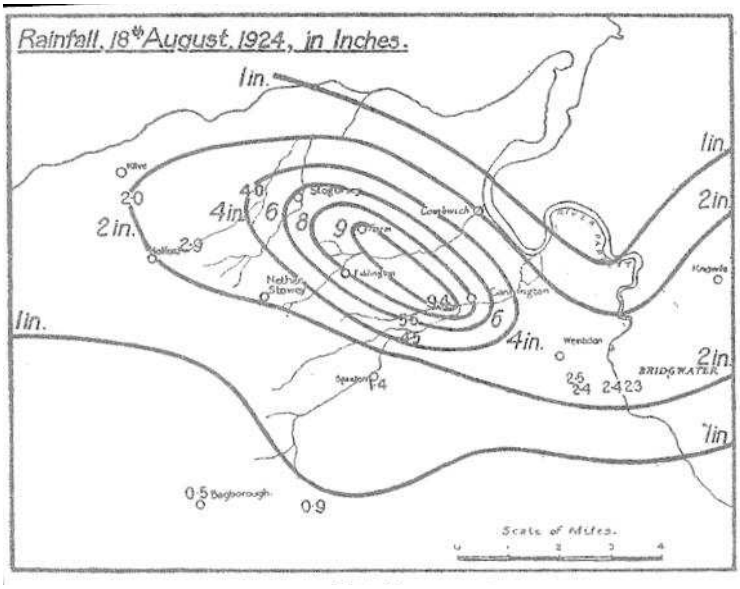

Figure 5. Storm isohyet map of heavy rainfall extent in Somerset, 18-19th August 1924 (from Glasspoole, 1924)

2.3 Current day extreme rainfall estimates at Hinkley Point

EDF have requested that estimates of rainfall depths be obtained for 15-minute, 1-hour and 24-hour durations for return periods of 1 in 100, 1 in 1,000 and 1 in 10,000 years. These have been extracted from the FEH under the guidance provided in Volumes I and II of the FEH (Reed, 1999 and Faulkner, 1999 respectively) and the results are summarised in Table 2. Additional rainfall estimates for lower return periods have also been provided for completeness and verification purposes.

Return Period/ Duration	Point Rainfall Estimates (mm)		
	15-minute	1-hour	Daily
1 in 2 years	8.6	13.5	40.3
1 in 5 years	12.8	18.6	50.4
1 in 10 years	15.7	23.0	58.4
1 in 100 years	33.3	44.6	92.6
1 in 1,000 years	69.5	85.5	145.6
1 in 10,000 years	145.1	163.7	228.8

Table 2. FEH Rainfall return period estimates for Hinkley Point (obtained using AMAX records, at a point location for a sliding duration[2])

The data in Table 2 illustrate the typical trends expected in return period analysis; rainfall depths increase with duration and return period. The most commonly applicable method

[2] Storm totals are accumulated for any start time in a 24-hour period. This reflects reality more closely as storm events may traverse the fixed measuring periods (i.e 09-09 GMT) used at gauging sites.

with which to verify the FEH rainfall estimates is to use nearby rain gauge records. The rain gauge data already described will be used to this end, however since the records exist only at a daily duration, only the daily duration estimates obtained from the FEH will be verified.

In order to obtain rainfall estimates from the observed historic data for the various return periods in Table 2, rainfall frequency analysis has been applied to both the Cannington/Brymore and Whitewick farm records using the Gringorten formula for plotting position (Equation 1) in association with the Gumbel Extreme Value relationship (GEV, with the AMAX values plotted against the reduced variate as demonstrated by Equation 2 and Table 3). The choice of this methodology is appropriate as the FEH estimates are also based on analysis using the Gumbel reduced variate. The following analysis compares the return period estimates from the observed data against FEH estimates obtained for the nearest 1 km grid-point to each rain gauge and then against the FEH estimates for Hinkley Point.

Equation 1

$$P(X) = \frac{r - 0.44}{N + 0.12}$$

Equation 2

$$y = -\ln\left[-\ln\left(1 - \frac{1}{T}\right)\right]$$

Return Period (years)	Reduced Variate
1 in 5	1.5
1 in 10	2.3
1 in 100	4.6
1 in 1,000	6.9
1 in 10,000	9.2

Table 3. Values of reduced variate for each return period

2.3.1 Cannington/Brymore

The initial analysis included the complete time series of AMAX records from 1905 to 2008. The resultant plot of rainfall depths against the reduced variate did not produce a

strong straight line fit (Figure 6). The data included the 1924 rainfall event for which the rainfall depth value far exceeded the distribution of the rest of the data set, and was found to introduce a bias into the results. The best straight line fit to the data is shown in Equation 3.

Equation 3

$$y = 16.732x + 29.539$$

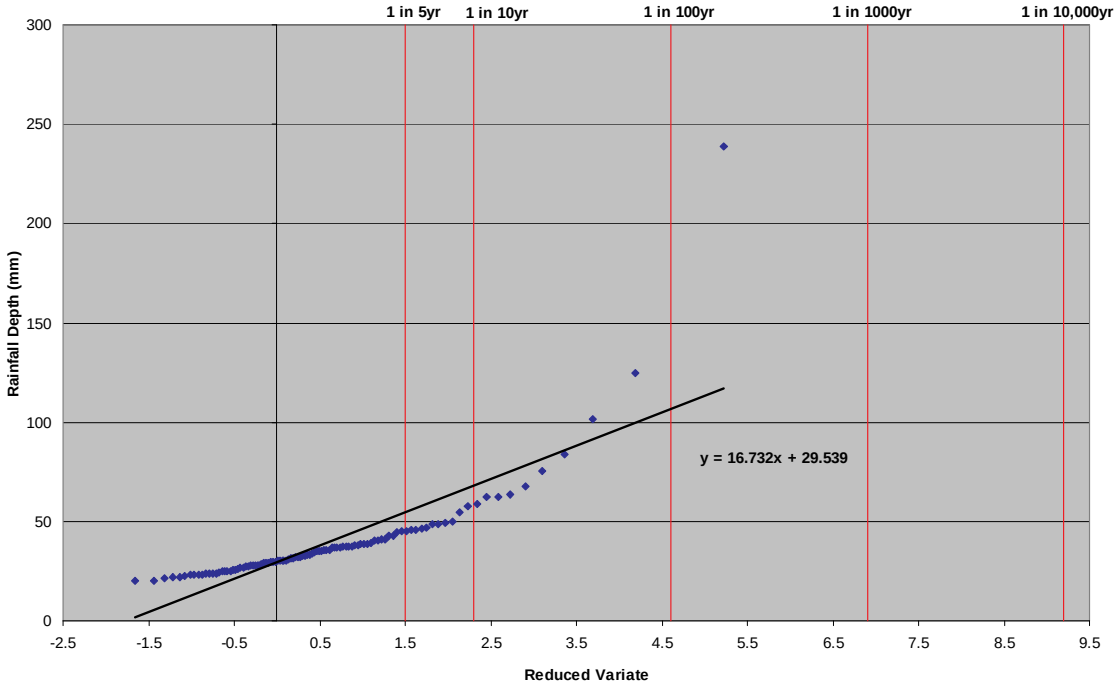

Figure 6. Gumbel plot of rainfall estimates at Cannington-Brymore 1905-2008 (incl. 1924 event)

Calculating the return period of the maximum event from Equation 3 suggests it was in the order of 1 in 200,000 years. Where such an extreme value occurs within a series, such as in this case, it is theoretically justified to treat it as independent of the historic data series therefore removing it from further analysis. This allows the return period of rainfall to be considered against the AMAX series, without introducing bias, and may produce a better independent estimate of the return period of the particular extreme event.

By omitting the maximum event from the AMAX series, the best fit line improves, but has a much lower slope, and the estimated return period for the maximum event is in the order of 1 in 10,000,000 years. The inability to plot a single straight line through the

points because of this outlier means it is difficult to calculate return periods with any confidence.

Further consideration of the amended plot, shown in Figure 7, would suggest that a 2-line relationship provides the best fit to the plotted series. Lines of best fit have been fitted to data points selected by eye to demonstrate these two relationships.

The relationship for the lower part of the line is given by Equation 4 and the upper part Equation 5:

Equation 4

$$y = 8.7437x + 30.277$$

Equation 5

$$y = 23.62x - 0.9113$$

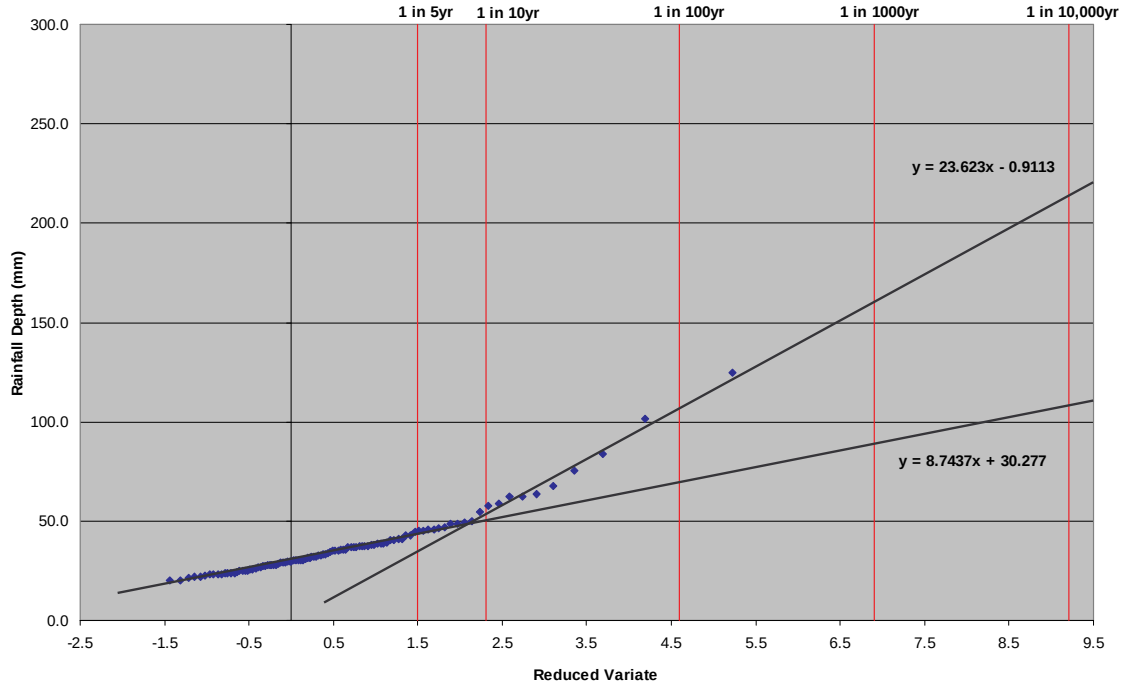

Figure 7. Gumbel plot of rainfall estimates at Cannington/Brymore 1905-2008 (omitting 1924 event)

Comparing the 1924 maximum value with the upper best-fit line (Equation 5), provides an estimated return period for that event in the order of 1 in 20,000 years. This is a much

more realistic return period given the rainfall depth and is in line with the results from the Reservoir Safety Project (Stewart et al., 2010) which has provided further information on the upper bounds of extreme probability relationships. Given the prominence of the two trends in the plotted time series both lines have been combined to provide the most confident final estimates for the selected return periods and these results are summarised in Table 4. Also included are the rainfall estimates obtained from FEH for the nearest 1km grid point to Cannington (NGR 325535E 139852N), for a fixed duration[3].

Return Period for daily duration	y = 8.7437x + 30.277	y = 23.623x - 0.9113	FEH estimates (fixed duration)
1 in 5	43.4		47.1
1 in 10	50.4		54.7
1 in 100		109.6	87.0
1 in 1,000		163.9	137.2
1 in 10,000		218.2	216.2

Table 4. Results of Gumbel return period analysis and FEH estimates at Cannington/Brymore

The results suggest that both Equation 4 and the FEH estimates reflect the rainfall depths well at lower return periods. The upper line (y = 23.623x - 0.9113) and the FEH estimates are somewhat different at the 1 in 100 and 1 in 1,000 year return periods, but are almost identical at the 1 in 10,000 year level. In combining the two curves, estimates are similar for return periods at 1 in 5, 10 and 10,000 years with differences at these return periods ranging from between 2.0 and 10.8 mm.

Estimates for the 1 in 100 year and 1 in 1,000 year events are not as consistent, with differences from FEH estimates of 22.6 mm and 26.7 mm respectively. These differences are not significantly large but do suggest that the FEH estimates are under-estimating rainfall depths at this site for these return periods. Some confidence can be attributed to this assertion given the particularly long record available for analysis, which should be considered when comparing the results from this analysis with FEH results obtained from Hinkley Point itself.

[3] The fixed duration estimates provide a rainfall depth over a discrete time interval in this case a 24 hour period, and therefore are comparable with the rain gauge data used in the analysis, which were measured daily at 0900z GMT.

2.3.2 Whitewick Farm

The Whitewick Farm record may be considered as typical of a moderately long data set, but one which does not contain any exceptional events (i.e.1924 and 1917) as recorded at Cannington/Brymore. As the closest daily rain gauge to the Hinkley Point site, it would be accepted good practice to analyse this annual series to compare with design rainfall estimates using FEH methods as has been carried out above using the Cannington/Brymore record.

The data plotted using the Gumbel analysis was such that a strong line of best fit could be fitted to the points, described by Equation 6 below and shown in Figure 8. Table 5 summarises the daily return period estimates obtained using this line of best fit for the Whitewick record and the estimates made using FEH for Whitewick Farm at the nearest 1km grid point (NGR 323600E, 145300N), for a fixed duration.

Equation 6

$$y = 16.217x + 7.3574$$

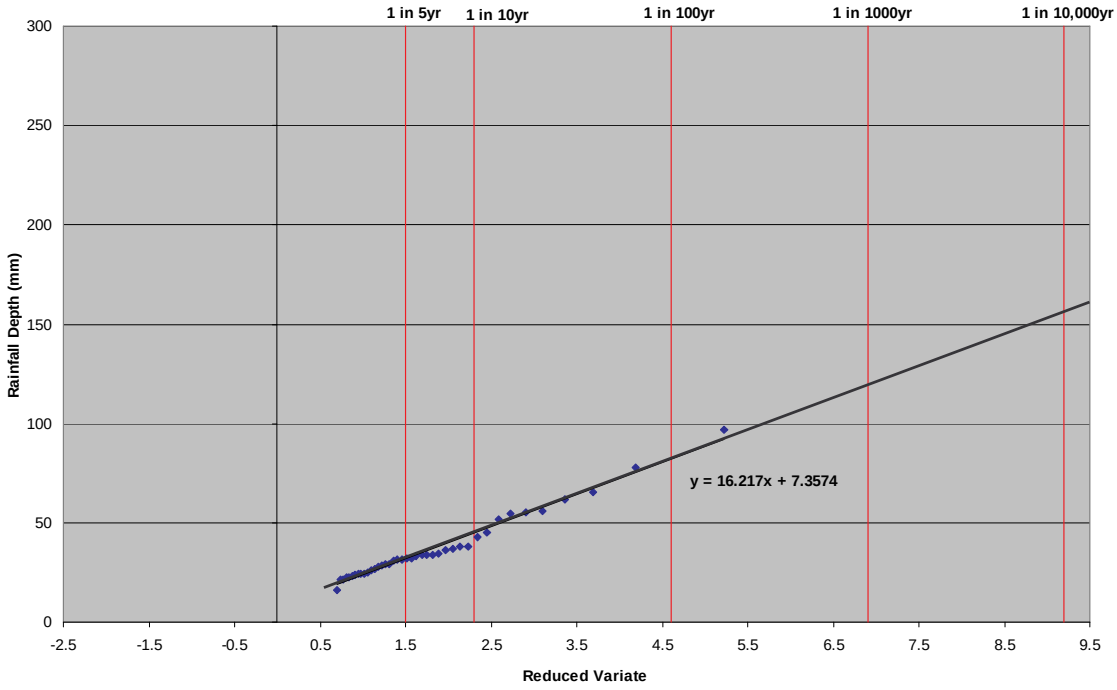

Figure 8. Gumbel plot of rainfall estimates at Whitewick Farm 1961-2001

Return Period for daily duration	Best Fit Line	FEH estimates (Fixed duration)
1 in 5	31.7	43.5
1 in 10	44.7	50.5
1 in 100	82.0	80.7
1 in 1,000	119.3	127.8
1 in 10,000	156.6	202.2

Table 5. Results of Gumbel return period analysis and FEH estimates at Whitewick Farm

The results suggest a good agreement between rainfall depths calculated in FEH and by the Gumbel analysis for return periods of 1 in 10, 100 and 1,000 years. However the 10,000 year return period results diverge considerably from each other, a difference of 45.6 mm between the two estimates (the FEH estimate being the greater of the two) which could have a considerable impact if used in storm drainage design specifications. At the 1 in 5 year return period, where the estimates would be expected to be very similar because of the data available to construct the estimates, there is a difference of 11.8 mm (the FEH estimate again is the greater of the two). These differences will inevitably arise, as the FEH method uses a "pooling" algorithm, where values from other stations within a varying radius of the point of interest, are used.

Given the length of the time series at Whitewick Farm it has provided a reasonable check of the FEH estimates which, in summary, have consistently over-estimated rainfall depths compared with the gauged records at this location. The FEH methodology is likely to capture a wider range of storm events from the areas surrounding Whitewick and thus provide a more reliable estimate of the extremes over longer return periods. Naturally it should also include some degree of influence of the Cannington/Brymore record (thus including weighting from the more extreme events), though the extent of this cannot be ascertained.

2.3.3 Comparison of FEH estimates with observation estimates

The results of the above analyses have demonstrated that the gauge records and FEH estimates for Cannington/Brymore and Whitewick Farm and reasonably similar. Therefore it is reasonable to use the gauged records to compare against the original FEH estimates for Hinkley point (Table 6) to assess the validity of these estimates.

The rainfall depth estimates for Hinkley point have been extracted from the FEH for Hinkley Point on a sliding duration. The return period results for Cannington/Brymore and Whitewick Farm are based on daily rainfall totals and therefore for a discrete fixed 24-hour duration, 09hrs-09hrs, as mentioned already. Based on extensive analysis of temporal patterns of sub-daily rainfall, the FEH has arrived at a correction factor (1.16) to convert daily fixed duration rainfall depths to a sliding duration. To compare with the FEH estimates for Hinkley Point (in Table 2) which have been extracted for a sliding duration, rainfall depths calculated from Cannington/Brymore and Whitewick Farm have been converted using the appropriate FEH factor (1.16). This allows a direct comparison of the three data sets. The results are presented in Table 6 and Figure 9 below.

Return Period	Hinkley Point FEH	Cannington/Brymore (sliding duration)	Whitewick Farm (sliding duration)
1 in 5	50.4	42.1	36.8
1 in 10	58.4	64.0	51.9
1 in 100	92.6	127.1	95.1
1 in 1,000	145.6	190.1	138.4
1 in 10,000	228.8	253.1	181.7

Table 6. Comparison of return period rainfall estimates at Hinkley Point Power Station, Cannington/Brymore and Whitewick Farm

Overall, the FEH estimates for Hinkley Point are generally well supported by the results shown by the extreme probability analysis for the Cannington/Brymore and Whitewick Farm rain gauge records.

Estimates are most closely reflected by the Whitewick Farm record with the exception of the 5 and 10,000 year return periods which are underestimated by the gauged record. This is to be expected however as the Whitewick Farm record is only 44 years long and is less likely to include extreme storm events. The Cannington/Brymore results show some more significant differences in the estimates. Whilst FEH estimates at 1 in 5 and 1 in 10 year return periods are well represented in the gauged records, estimates at 1 in 100, 1,000 and 10,000 year return periods are greater than the FEH results (34.5, 44.5 and 24.3 mm respectively). This emphasises the influence of the two major events in the Cannington/Brymore record and also indicates that the FEH is under-estimating extreme rainfall at this location.

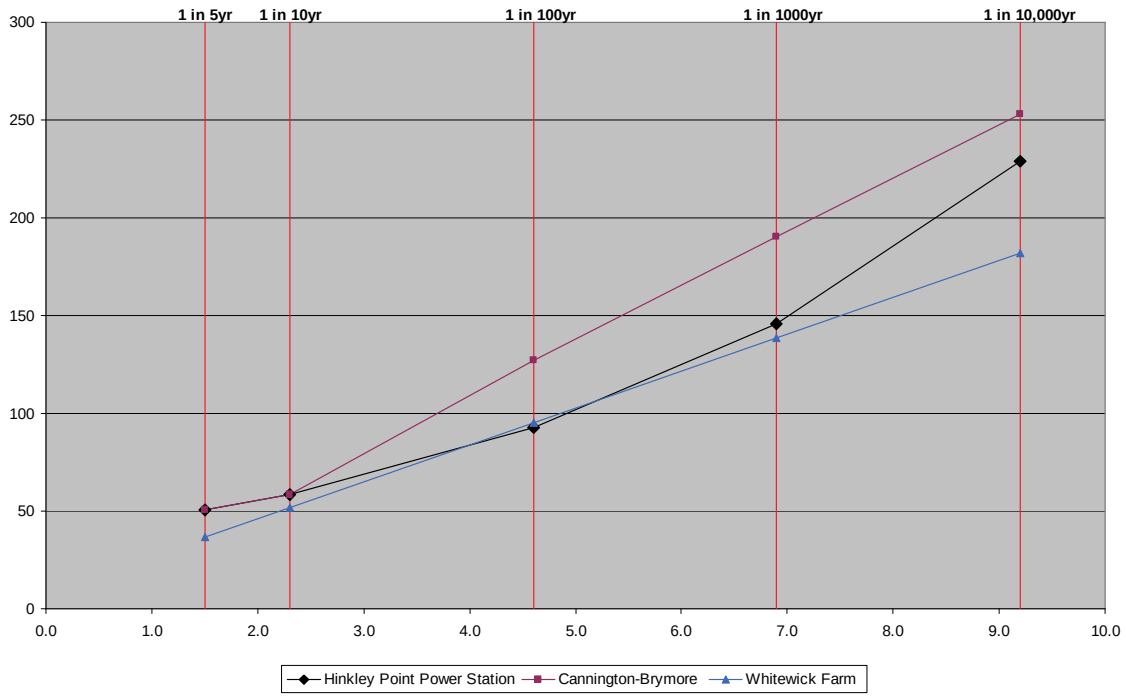

Figure 9. Comparison of return period rainfall estimates at Hinkley Point Power Station (FEH estimates, sliding duration), Cannington/Brymore and Whitewick Farm (Gumbel estimates, sliding duration)

Although there are discrepancies between the two records and the FEH estimates, the FEH estimates fall within the bounds of both individual station probability analyses. Given the length of the record at Cannington/Brymore and the close proximity of both sites to Hinkley Point they provide confirmation of the estimates produced using the FEH for daily storm durations.

Perhaps the most important conclusion is that the FEH 10,000-year estimate for Hinkley Point Power Station, is not significantly different from the observed event in 1924, which gives confidence to the magnitude of a maximum design rainfall. In the Reservoir Safety Study (Stewart et al., 2010), the storm total has been estimated as having a return period of between 13,000 and 14,000 years, and the recorded rainfall of 238.8mm exceeds the FSR (NERC, 1975) estimate of probable maximum precipitation (PMP) for that locality and duration, which is 218mm. Consideration of estimating PMP and its implication with regard to the RCM estimates, is covered in Section 6.

3. Analysis of precipitation from observations and RCM estimated extreme precipitation for the current climate

The objective of this study is to provide estimates of extreme rainfall at Hinkley Point into the future, taking into account the effects of projected climate change. In order to provide a quantitative estimate of the impact of climate change, the daily rainfall data input into the UK Climate Projections (UKCP09) have been analysed. A full description of the climate models and the methodology used to create the UKCP09 projections is given elsewhere (Buonomo et al., 2007, Murphy et al., 2009), and so only a brief summary is given here.

3.1 Regional Climate Model simulations

The UKCP09 climate projections (Murphy et al., 2009) were generated using the Met Office Hadley Centre's regional climate model HadRM3. This regional climate model (RCM) covers Europe and parts of the North Atlantic Ocean and has the same structure as the atmospheric component of the global climate model HadCM3 (Gordon et al., 2000), with the same vertical level spacing (19 levels, which represent the atmosphere between the surface and approx. 10 hPa), but has a much higher horizontal resolution (25 km). Regional climate models simulate climate over smaller scales, such as over continents, compared with global climate models, and so boundary conditions of key meteorological variables (such as wind speed and direction, humidity and temperature) are needed at the edges of the model domain. The boundary conditions used were taken from existing global climate model simulations, which had been stored at 6 hourly intervals. These boundary conditions are used by the RCM to provide the required meteorological data at every model time step (30 minutes). The climates simulated by the global climate model and the RCM over the UK will be essentially the same at scales resolved by the global model. The RCM adds detail to the selected region, but is constrained by the global model providing the boundary conditions.

Climate models are, in essence, a mathematical representation of the atmosphere, and contain many equations based on physical principles. Our knowledge of the atmosphere and all the different processes which occur in it is incomplete, and, owing to the finite resolution of the model, some key processes cannot be represented explicitly. For example, the flow of air upwards and over hills, convection and cloud formation, are important for modelling of rainfall, and take place at spatial scales smaller than the

model resolution. They must be estimated using relationships with variables such as wind, temperature and humidity calculated at the scale of the model (here, 25 km). These relationships are called parameterisations. The nature of the equations used in the model mean that values for many parameters must be specified. Precise values for some parameters are difficult to obtain, and so their validity is uncertain.

In order to explore the impacts of these uncertain parameters on the modelled climate, 16 global climate model simulations (collectively called an ensemble) were generated in which many of these uncertain parameters were changed slightly from their standard values. An additional simulation where all parameters had their standard values was also run. Further details are given by Collins et al. (2006). This set of 17 global climate simulations were used to provide boundary conditions for 17 RCM simulations of the present and future climate of the UK. Each RCM had the same set of parameter values as the global model used to provide the boundary conditions. However, an analysis of the RCM climates showed that the simulations of storms and precipitation in 6 of the RCMs were unacceptable (Murphy et al., 2009, Chapter 5), and so only climate data from the remaining 11 RCM simulations were analysed further. These 11 RCM simulations are identified by letters: X is the control run, and the others are A, C, H, I, J, K, L, M, O and Q. The climate projections from these simulations are referred to as the 11-member RCM ensemble, and were released alongside the UKCP09 climate projections. They were generated using a medium emissions scenario (A1B; IPCC, 2000). The UKCP09 projections also show results using a high (A1FI) and low (B1) emissions scenarios, but raw model data for these latter scenarios are not available.

3.2 Methodology

The RCM grid square containing Hinkley Point was identified using the OS grid reference for Hinkley Point (321000 E and 146000 N). However, the grid square identified is classed as ‘sea’ by the RCM (most climate models assign grid squares to either land or sea). Projections of extreme rainfall for this grid square would not therefore be appropriate for this study so data from the closest grid square to Hinkley Point classified as ‘land’ (the white square in Figure 10) were extracted.

In order to assess the performance of RCM projections for Hinkley Point in the future, the RCM output produced for 1949 to 2008 has been compared against observed datasets from the same area to see how well the RCM has replicated the statistics of

rainfall observations. The observed datasets include the daily rain gauge data for Cannington/Brymore from 1961 to 2008, Whitewick Farm from 1961 to 2001 and the National Climate Information Centre (NCIC) daily rainfall gridded datasets from 1958 to 2007. NCIC daily rainfall data are available at a resolution of 5 km and are calculated using a regression model using measured rainfall data from the UK rain gauge network and known factors that affect them, such as altitude, latitude and longitude, distance to the coast etc. The interpolation methods are described in more detail by Perry and Hollis (2005).

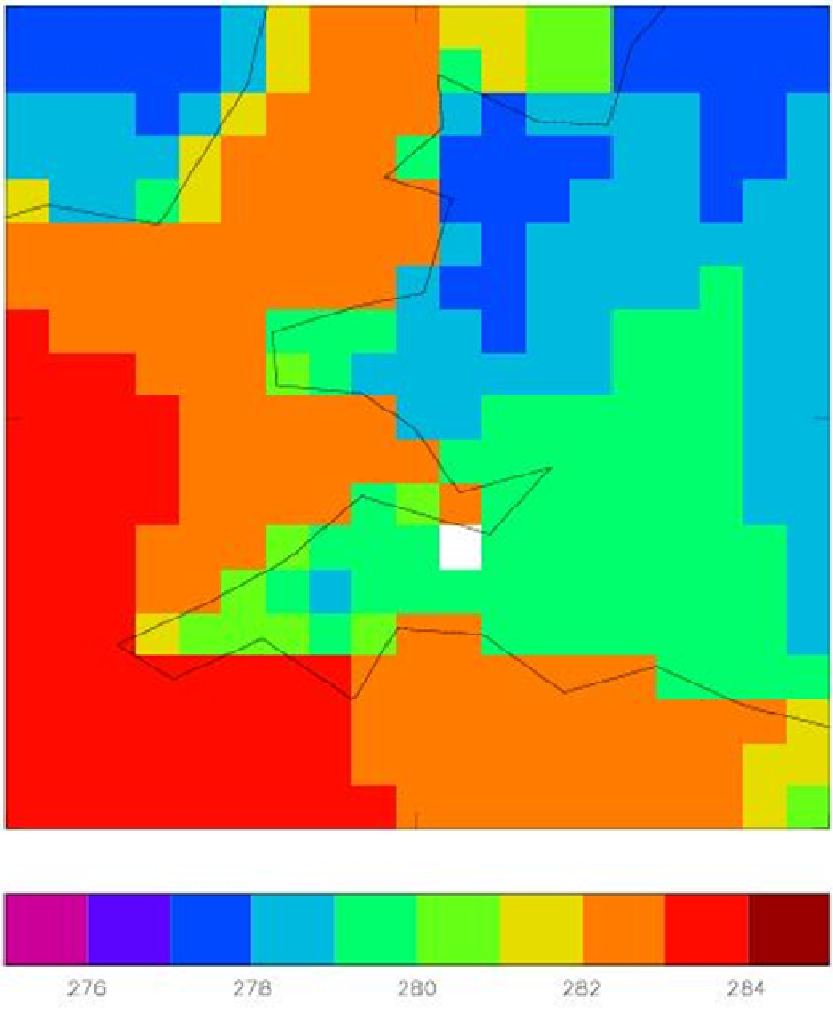

Figure 10. Location of the RCM 25km x 25km grid square (white) chosen in reference to Hinkley Point

In order to be comparable with the RCM data, the daily rainfall data from the 5 km gridded dataset produced by the NCIC have been aggregated to the 25 km x 25 km grid used by the regional climate model. These 25 km data have been produced to support the UKCP09 climate projections.

A preliminary assessment has been conducted to assess the statistical similarity of the three data sources (Section 3.3). The datasets have been fitted to an extreme value distribution – the Marked Point Process distribution, then estimates of rainfall depths at varying return periods has been made (Section 3.4). These results have then been compared to assess the performance of the RCM output and the results from all three data sources have been compared with FEH estimates as a verification of the results.

3.3 Time Series Analysis

The basic descriptive statistics of the different observed and RCM generated time series data have been compiled, and these are presented in Table 7, Table 8 and Table 9.

	Cannington/Brymore (1961-2008)	Whitewick Farm (1961-2001)	NCIC 25 km (1958-2007)
Mean	2.1	2.1	2.4
Median	0.0	0.0	0.3
75%ile	2.2	2.3	2.7
99%ile	20.3	19.5	20.9
Skewness	4.7	4.7	4.2
Maximum	102.0	97.0	105.6

Table 7. Summary of the distributions of observed daily rainfall

A comparison of the data in Table 7 indicates that the distributions of the three observed datasets are very similar as the difference between the statistics is minimal. Whilst the difference between the means of the datasets is only 0.3 mm the median is a more robust measure of the centre of the distributions as it is not influenced by the extremes in the datasets. The median for Cannington/Brymore and Whitewick Farm indicates that a greater proportion of daily rainfall values recorded no rainfall compared with the NCIC gridded data. This is to be expected as the NCIC data are an interpolation of multiple rain gauges within and on the periphery of a 25 km x 25 km grid square and so are likely to capture more rainfall events than would be recorded at a single point.

All three distributions are very positively skewed and the nature of the skew is typical of a large population of daily rainfall data, where the majority of values are zero or low magnitude. Representative statistics of the extremes in each time series are the values given in Table 7 for the 75th and 99th percentile which provide an indication of the similarity between the datasets at the upper end of each distribution. Threshold values at both percentiles are very similar, with a difference of 0.5 and 0.6 mm at the 75th and 99th percentile respectively between Cannington/Brymore and the NCIC data. Combined with

the maximum value for these datasets, which are different by only 3.6mm, the upper ends of the both distributions show an almost identical relationship. Of interest is that the 99th percentile value and maximum rainfall for Whitewick Farm are slightly lower, which suggests that the values in this area of the distribution are lower than the Cannington/Brymore and NCIC datasets.

	RCM_A	RCM_C	RCM_H	RCM_I	RCM_J	RCM_K
Mean	2.1	2.1	2.4	2.2	1.9	1.9
Median	0.3	0.4	0.5	0.4	0.2	0.3
75%ile	2.5	2.5	2.9	2.7	2.3	2.3
99%ile	18.2	17.5	21.6	17.9	16.5	15.8
Skewness	3.5	3.8	4.0	3.3	3.2	3.6
Maximum	53.4	64.0	82.8	66.4	45.2	58.7

Table 8. Summary of the distributions of the RCM runs A-K for daily rainfall (1949-2008)

	RCM_L	RCM_M	RCM_O	RCM_Q	RCM_X
Mean	2.2	2.4	2.4	2.1	2.4
Median	0.4	0.5	0.6	0.4	0.5
75%ile	2.7	3.0	2.9	2.5	3.0
99%ile	18.4	19.9	19.2	17.7	20.0
Skewness	3.2	4.6	3.4	3.4	4.3
Maximum	45.2	125.6	52.7	56.9	116.5

Table 9. Summary of the distributions of the RCM runs L-X for daily rainfall (1949-2008)

In contrast to the observed rainfall data, the summary data in Table 8 and Table 9 indicate considerable variation between the derived RCM datasets. Mean values vary from between 1.86 and 2.44 mm. The median suggests the distributions have greater similarity, values range from between 0.23 and 0.60 mm.

A comparison of the 75th, 99th percentiles and the maximum rainfall depth for each model run indicates that there is some variability between the datasets at the upper ends of each distribution. The maximum values vary considerably; the difference between the smallest and largest maximum is 80.4 mm which is a considerable range. It is particularly important in achieving the aims of this study that the RCM runs reflect the

observed extremes in daily precipitation accurately so that a realistic estimate of the "change factor" can be produced for precipitation with large return periods up to 10,000 years. A comparison of the three summary tables demonstrates that only RCM runs M and X produce maximum rainfall of similar depths to the observed records. The other RCM runs fall short of producing the large rainfall depths recorded in the observed records. There are several possible explanations for this. The RCM produces estimates of rainfall over large grid boxes and in order for rainfall amounts to be recorded in individual boxes, storm events generated in the model must traverse multiple grid boxes and therefore localised rainfall events, which occur more frequently in reality and are often more intense, are not well represented in the RCM. In addition, the model produces average rainfall for a 25 km x 25 km area which will be less than observations recorded at a point. In summary the analysis of the rainfall estimates for the RCM generated datasets in Section 3.1 for long return periods are unlikely to accurately reflect the observations.

3.4 Analysis of Extreme Events

When considering the frequency and severity of extreme events, a simple cumulative frequency analysis could be conducted. The modelled and observed data may be used to construct cumulative frequency distributions, and an extreme event could be defined as, for example, all events in the top 5% of the data. However, it is impossible to estimate the probability of occurrence of an extreme event of greater magnitude than the maximum in the data series from a cumulative frequency distribution. The threshold used to identify an extreme event is also fairly arbitrary; consequently, the number and frequency of extreme events obtained from a cumulative frequency distribution is likely to be strongly dependent on the threshold choice. Other problems arise, because the observations used may not be sufficiently long enough to ensure all previous extreme events have been captured. For example, a 50 year record is inadequate when looking for 1 in 100 year events, and even more so for 1 in 10,000 year events. There may also be gaps in the observations, and so some extreme events may not have been recorded. Similarly, extreme events are often localised and so some could be missed by the rain gauge network. Extreme value analysis is not subject to the limitations of a cumulative frequency analysis, and is therefore the methodology that has been used here. It is described in more detail in section 3.5.

3.5 Extreme Value Analysis

Extreme value analysis (EVA) is a statistical method that can be used to estimate the probability and severity of events that are more extreme than any that exist in a given data series. EVA may be used to estimate the probability and severity of future events based on a limited set of data. For example, a 30 year observation record could be used to estimate extreme events over the next 100 years (Coles, 2001). It also allows estimation of a suitable threshold for the identification of extreme events and their return periods. It is important to remember that the uncertainty in the projected extreme events will increase as the return period approaches the length of data available, and increases still further as the return period exceeds the length of the data series.

3.5.1 EVA Methodology

There are many different statistical models which can be used for extreme value analysis. In this report, the Marked Point Process (MPP) distribution has been used, which is a different method to that used in Section 2 of this report. The MPP distribution only considers events with magnitudes (rainfall depths in this case) above a specified threshold, i.e. it is a peak-over-threshold (POT) approach, rather than an annual maximum series (AMAX) approach. This distribution has two components: a Poisson process which models how many times an extreme threshold is exceeded and a Generalized Pareto distribution which models by how much the threshold set by the Poisson distribution is exceeded. A MPP distribution has three parameters; location, scale and shape, which are given the symbols μ, σ and ξ respectively. The location parameter is analogous to the mean of a normal distribution in that an increase in the location parameter results in the entire distribution being shifted to the higher values but the shape of the distribution remains unchanged. The scale and the shape parameters together measure the rate at which the magnitudes of the extremes alter with lengthening return period. The expected number of exceedances per year of value x, given x is greater than a threshold u, may be found using Equation 7 (Coles, 2001):

Equation 7

$$\left[1+\xi\left(\frac{x-\mu}{\sigma}\right)\right]^{-1/\xi}$$

This formulation of the marked point process (MPP) model ensures that the scale parameter is invariant to the threshold u. The MPP parameters are estimated by maximum likelihood (see Appendix, section 9.3). From this model, the return level (z_m) experienced on average every *m* years (or, an event which has a probability of 1/*m* of occurring in any year) may be calculated using Equation 8 (Coles, 2001):

Equation 8

$$z_m = \mu - (\sigma / \xi)\left\{1 - \left[-\ln\left(1 - \frac{1}{m}\right)\right]^{-\xi}\right\} \quad given \quad \xi \neq 0$$

An example of an EVA curve fitted to maximum temperature data, together with the effect of altering each of the location, scale and shape parameters, is given in Figure 11 (reproduced from Brown et al, 2008).

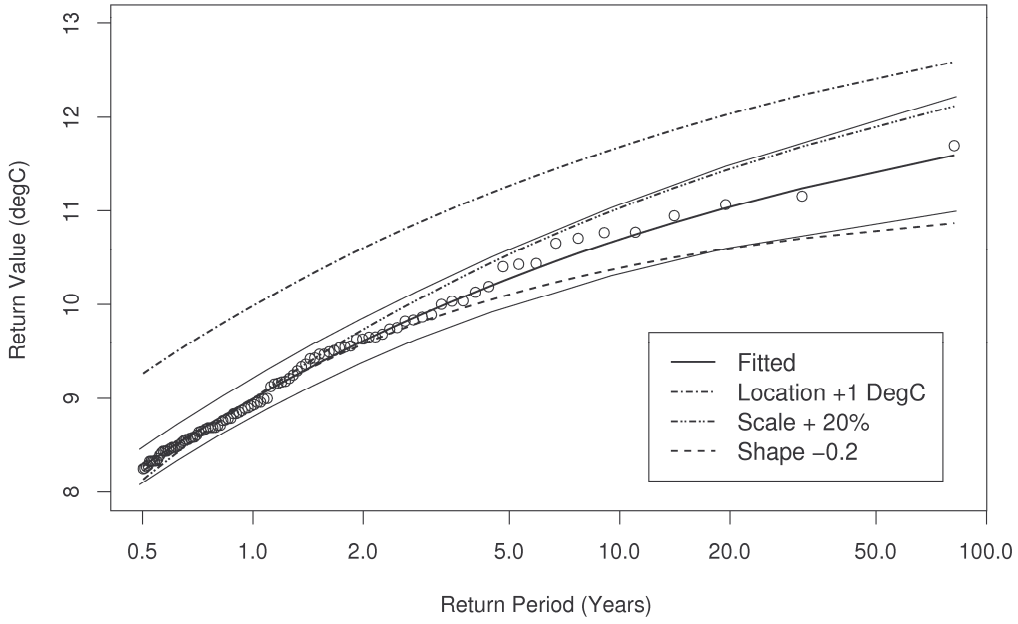

Figure 11. Return level curve derived from fitting a marked point process to the extreme (>98.5%) daily maximum temperature for the grid box containing London. Circles represent return levels derived from the data, the solid black line is the fitted values using the derived MPP distribution with associated 5-95% confidence intervals (lighter solid lines). Non-solid lines represent return-level curves where the distribution parameters are adjusted as described in the legend. Reproduced from Brown et al. (2008).

The thick solid line shows the fitted curve and the two thin solid lines the parametric uncertainty estimates. Increasing the location parameter moves the whole curve up the y-axis but does not change its shape. Increasing the scale parameter effectively rotates

the curve about a point, changing the rate at which extreme values will change with increasing return period, but does not change the shape of the curve. Reducing the shape parameter increases the degree of curvature, which, in the example shown in Figure 11, means that extreme values at larger return periods (e.g. 1,000 years) will only be slightly greater than those for a 100 year return period.

EVA has been carried out on each of the RCM simulations for the period 1949-2008. Rainfall depths at varying return periods have been calculated by fitting each dataset to the MPP distribution. As this method uses the full record of daily rainfall, including all events above the threshold (here, the 99th percentile), there is more information available for analysis (see Figure 12).

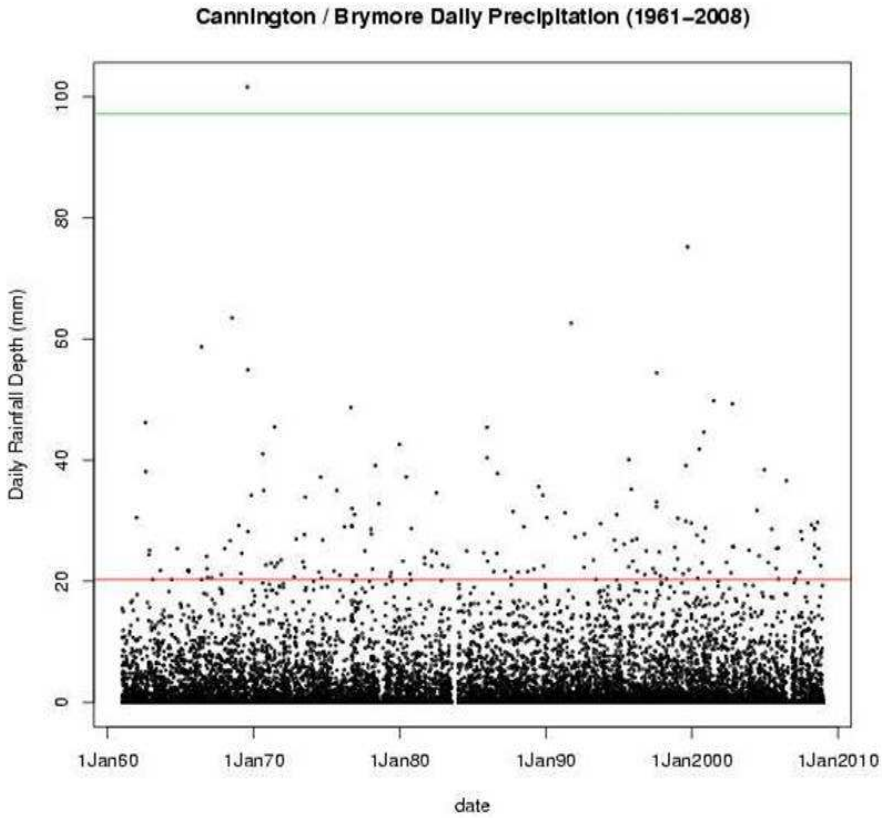

Figure 12. Example plot showing the 99% threshold (red line) and 50 year return period estimate (green line) constructed by fitting the data to the MPP distribution

This means that the shape parameter (a value which describes the shape of the best fit line fitted to the data points, see Figure 13), which is critical when extrapolating to return periods such as 10,000 years, can be estimated with greater accuracy than when using an annual maximum approach. The comparative analysis for Cannington/Brymore has only used data recorded after 1961, i.e. the daily digitised record. Thus the different

length of data set and the method of analysis will produce different results from those obtained in Section 2. Diagnostic plots suggest that the models are generally a good fit to the data (examples are shown in Figure 13). The shape parameter for most of the rainfall datasets is slightly positive, between 0.1 and 0.25, indicating an unbounded distribution with return levels increasing more quickly as the return period increases. Two of the RCM model runs (A and O) have slightly negative shape parameters, however, which would indicate a distribution which gradually levels off to an upper bound as the return period increases.

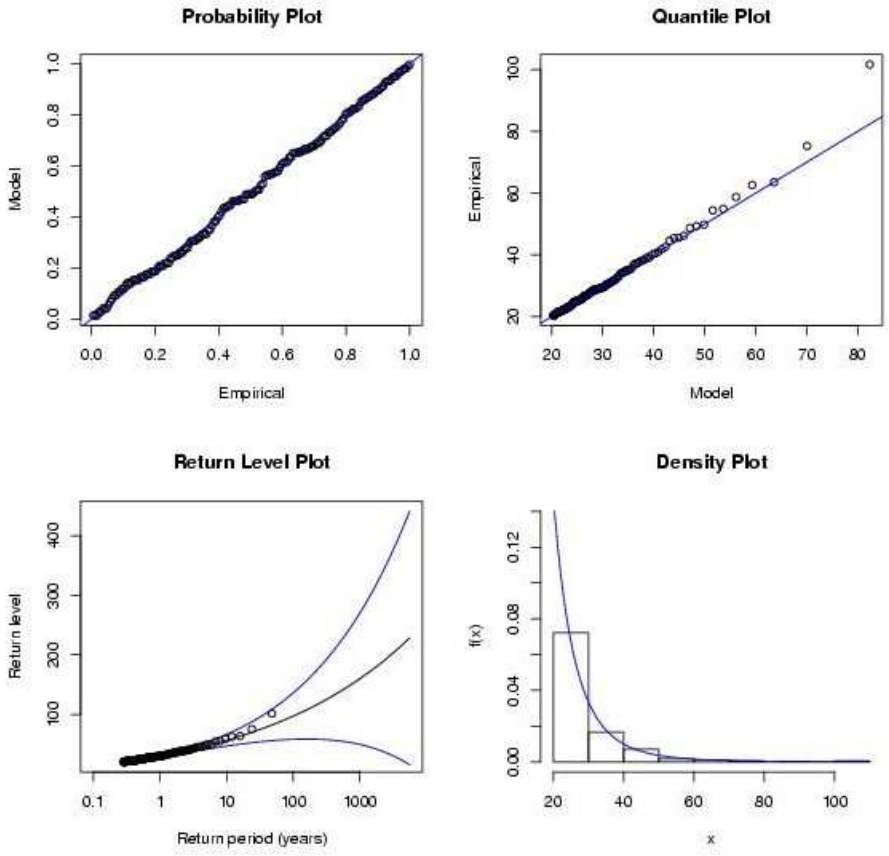

Figure 13. Example diagnostic plots from the EVA using the MPP distribution for Cannington/Brymore 1961-2008. The bottom right plot shows the best fit curve (and therefore an idea of the shape parameter) fitted to the data to provide the return period estimates.

3.5.2 Results from extreme value analysis

The results of the EVA are presented in Figure 14. This enables a comparison of the estimated rainfall depths using the observed records (Cannington/Brymore and NCIC gridded) and the 11 RCM datasets.

It is evident that the observed datasets (Cannington/Brymore, Whitewick Farm and the NCIC gridded dataset) produce very similar rainfall depth estimates up to the 100 year return period. The Cannington/Brymore and NCIC records produce almost identical 1,000 year estimates though the NCIC estimate is higher at 10,000 years by 29.5 mm. The Whitewick Farm record is slightly higher at the 1,000 year return period and considerably higher than the Cannington/Brymore and NCIC results with differences of 65.9 and 36.1 mm respectively. A likely explanation for the higher NCIC estimates versus the Cannington/Brymore record is that the NCIC dataset effectively incorporates a number of rain gauges over a 25 km x 25 km area and is therefore likely to include more extreme storm events than the Cannington/Brymore record which is only a point observation. The NCIC dataset is also a few years longer than the Cannington/Brymore record used for this comparison. This does not however explain the higher estimates produced by the Whitewick Farm record. The shape parameter applied when fitting the data to the MPP distribution is slightly more positive for Whitewick Farm (0.251) compared with the Cannington/Brymore (0.190) and NCIC (0.237) records. This has the effect of increasing the magnitude of estimates at the upper tail of the distribution and given that the datasets are very similar this is the most probable explanation.

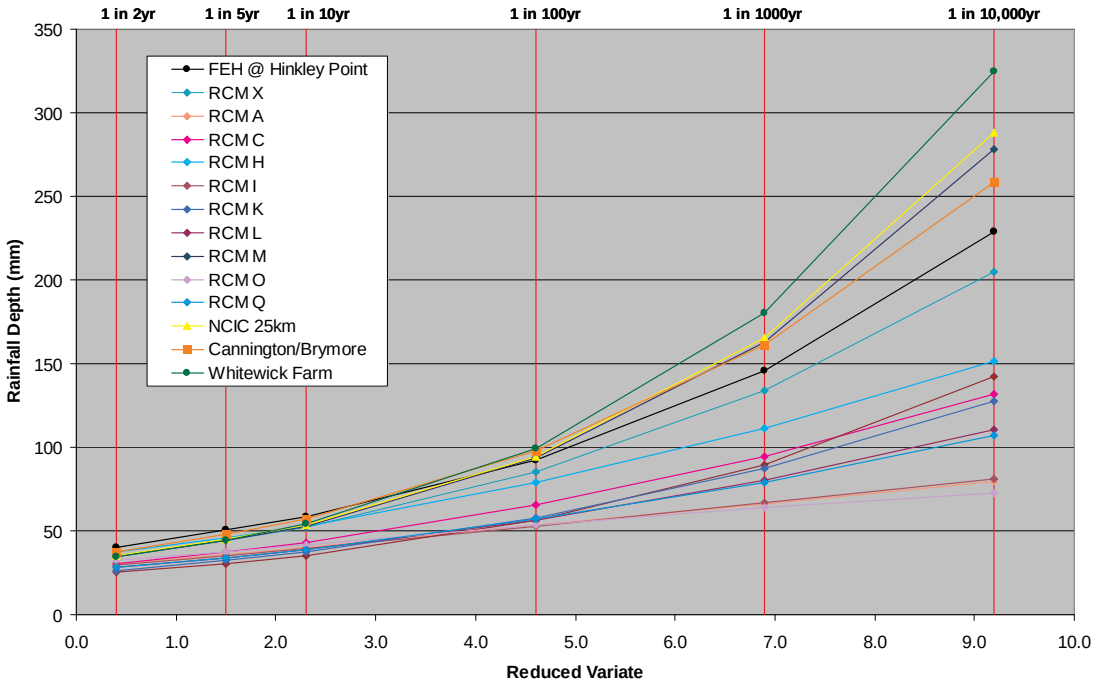

Figure 14. Present day rainfall return period estimates for observed and RCM datasets using the MPP distribution and FEH estimates at Hinkley Point

The overall trend in the estimates produced for almost all the RCM runs are a bias towards an underestimation of rainfall depths at all return periods compared with observed records. The one exception to this trend is RCM M, which closely replicates the observed data sets for rainfall depths out to the 10,000 year return period. RCM X produces depth values which are above those produced by the majority of the RCM runs and produces comparable estimates out to the 10 year return period, however beyond this, estimates are below those calculated from the observed rainfall data.

Generally, the error in depth estimates for the RCM runs increases as the return period increases. This is not altogether surprising given that estimates at return periods larger than 100 years are extrapolations beyond the bounds of the time series of data used in the analysis. The populations of data derived from each RCM run, except for RCM M, have underestimated rainfall depths up to the 10 year return period compare with observations but greater confidence at lower return periods. As discussed above, the RCM can only produce an average rainfall over each 25 km x 25 km grid square, and so will tend to underestimate observed extreme rainfall events in any case.

A further assessment of the results of the EVA using the MPP distribution can be made by comparing the rainfall estimates with the FEH results produced in Section 2.3, Table 2. The comparison in Figure 14 shows good agreement in rainfall depths between all datasets up to the 10 year (reduced variate = 2.3) return period. Beyond this the observed datasets and RCM M produce results which are in excess of the FEH estimates. This provides further support for the conclusion reached in Section 2 of this report which indicated that the FEH estimates at Hinkley Point may be an under-estimation of the potential rainfall depths at return periods of 1,000 and 10,000 years. This is further supported by other authors (see for example Clark, 1995 and 1997, MacDonald and Scott, 2000 and Kjeldsen et al., 2008). RCM X more closely reflects the FEH estimates at these extremes than either the observed records or RCM M. The remaining RCM results can be seen to considerably underestimate rainfall depths in comparison with the FEH results at the 100 year return period and beyond. These results suggest that the underlying parameters used to derive the RCM runs should be investigated further to explain the differences apparent between each RCM dataset.

4. Projected change in precipitation extremes using Regional Climate Model data

4.1 Initial analysis of modelled precipitation

The mathematical equations used to model climate in the RCMs incorporate many parameters, as discussed above. Here, ten parameters which potentially could change the modelled precipitation amounts were identified. The 11 RCM models were split into two groups depending on their values of the parameter selected. The particular models and the number of models in each group changed depending on the parameter under consideration. Several different precipitation metrics were calculated for the models, using data from the period 1961-1990. The metrics from each group were then compared to see if they were statistically different. Of the ten parameters examined, three were found to have a significant influence on modelled precipitation amounts. Six of the 11 RCM members have the same settings for these three parameters. It is reasonable to assume that these six members are sampling from a more similar distribution of precipitation than the other members. However, there is no way of knowing whether the distribution from these six members is more correct than a distribution from the other RCM members. The remaining 5 members are likely to produce different responses to the changing climate owing to the differences in the ten parameters. However, owing to the small number of models available, precipitation amounts from the 6 members with the same settings of the three parameters (which will be referred to as the six preferred RCMs) and all 11 members were analysed further.

4.2 Extreme Value Analysis

In this section, the EVA methodology is described, followed by a discussion of the RCM precipitation data and trends in observed precipitation amounts from observations. The basic methodology is the same as described in section 3.5, but with a modification to incorporate climate change influences.

4.2.1 EVA Methodology

These three parameters which define the MPP curve (location, scale and shape) are estimated using “maximum likelihood” methods (Coles, 2001; see the Appendix, section 9.3 for more information). When fitting MPP distributions the data are usually assumed

to be independent and stationary. The latter term means that the mean of the distribution doesn't change in a systematic way with time. When considering climate change this assumption is not true. However, an additional advantage of using the MPP distribution is that any non-stationarity can be modelled by allowing one or more of the three MPP parameters to depend on time (Kharin and Zweirs, 2005). The MPP parameters were assessed for non-stationarity, with respect to climate change, using likelihood ratio tests. The modified versions of the three parameters are given below:

Equations 9, 10 and 11

$$\mu = \mu_0 + \mu_t C(t) \qquad \sigma = \exp[\sigma_0 + \sigma_t C(t)] \qquad \xi = \xi_0 + \xi_t C(t)$$

C(t) represents a climate variable which changes with time, and is called the covariate. In this work, the covariate is global mean temperature. Precipitation is known to increase as temperatures rise, and so temperature is a suitable covariate for this work. Here, mean temperatures for the south-west region of the UK (using the same definition as UKCIP) were used as covariates. Any non-stationarity in the MPP parameters is found by fitting the MPP model, allowing one or more of the MPP parameters to change with the covariate. The model with a time-dependent parameter is deemed to be a significantly better description of the data than the same model with a time-invariant parameter if the deviance between the two models exceeds the 90th percentile of the chi-squared distribution with one degree of freedom (Coles, 2001).

Once the three parameters have been estimated, the quality of the fit of the MPP distribution to the data was assessed. Three different Goodness-of-Fit (GOF) statistics were calculated. The particular GOF statistics used were the Anderson-Darling test, Kolmogorov-Smirnov test and the Cramer-von-Mises test. These GOF statistics all assess slightly different aspects of the distributions. The Kolmogorov-Smirnov test looks at the MPP distribution derived from the data, and hypothesises that the data come from an MPP distribution. The alternative hypothesis is that the data are not from a MPP distribution. It is not specified how the data differ from the MPP distribution; it could have different location parameters, scale parameters or shape parameters. The test statistic is the greatest difference between the cumulative density function (CDF) for a MPP and that derived from the data. The Anderson-Darling test is a modification of the Kolmogorov-Smirnov test and gives more weight to the tails of the distributions. For the Cramer-von-Mises test, the data are not standardised and compared with a standard

normal distribution (as they are in the Kolmogorv-Smirnov test), as this process can make the GOF test less powerful.

Critical values of the GOF tests from which to determine confidence intervals cannot be derived analytically so a 'bootstrap' method is employed. New samples of extremes are derived from the fitted distribution which are then in turn submitted to the fitting and GOF test procedure. This is repeated 500 times to produce a distribution of GOF test values. The original fit is deemed to be a good fit of the data if the GOF value is less than the 90th percentile of the bootstrapped GOF values. Here, the Kolmogorov-Smirnov test statistic is used.

The exact threshold used to define an extreme event is almost always uncertain to some extent. The raw data to be analysed consist of a series of precipitation amounts, and those amounts above some threshold are considered extreme events. If the threshold is too low, there will be too many precipitation values which are not true extremes, and the asymptotic basis of the MPP model will be violated. However, if the threshold is set too high, there will only be a small number of extreme events with which the MPP model parameters may be estimated. This results in a large uncertainty in the parameter values. The standard practice of adopting as low a threshold as possible while still obtaining a good fit to the data has been used here.

4.2.2 RCM Data

The RCM data have a resolution of 25 km. The precipitation data from just one model point are unlikely to be exactly representative of that location. Extreme precipitation events may occur in adjacent model points which should be included in the analysis. For this reason, precipitation data from the model point which includes Hinkley Point, and three neighbouring model points (Figure 15), have been used. The three other points are all adjacent to the coast and the modelled precipitation amounts are similar to those from the point containing Hinkley Point. The data were pooled together to create a single dataset.

An analysis of observed rainfall amounts shows that UK rainfall has become more polarised between the seasons, with increased total rainfall in winter and reduced total rainfall in summer (Jenkins et al., 2008). Climate projections from UKCIP suggest that this trend may continue throughout the 21st century, although the exact impact on

summer rainfall amounts is uncertain. Some projections suggest that rainfall will occur in fewer but more intense storms in the future. Initially, rainfall amounts from all seasons were analysed together.

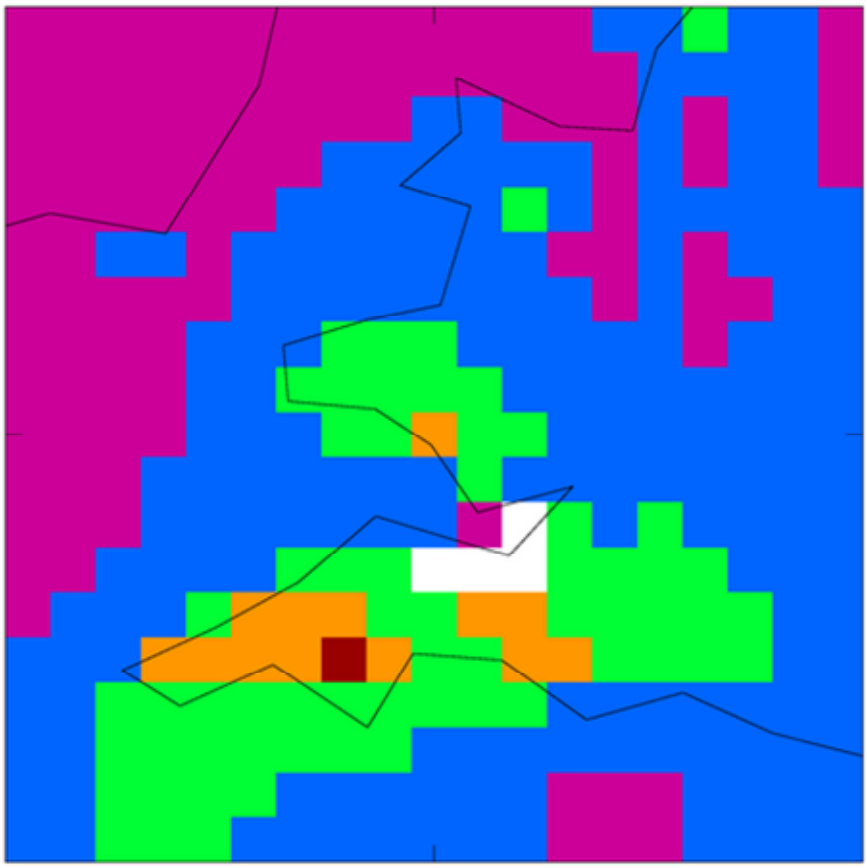

Figure 15. Location of four model grid squares around and including Hinkley Point (shown in white).

4.3 Results from Extreme Value Analysis

Initially, when performing the MPP analysis, only the location parameter was made a function of the covariate. This approach has been used successfully for analysis of extreme temperatures. Other research on results from global climate models indicates a linear dependence of precipitation on temperature (Lambert and Webb, 2008; Lambert et al., 2008). However, the modelled change in the 1 in 10,000 year extreme rainfall for Hinkley Point was small, and lay between 1 and 50 mm d^{-1}. There was little change in the location parameter, i.e. the climate change signal for this parameter is very low. An example of the increases in precipitation using the 6 preferred RCM members is shown in Figure 16. There is no clear maximum in the distribution, indicating that the “true” distribution is poorly sampled using just 6 RCM members; that is, there are large

differences in the extreme precipitation amounts from each RCM member, despite the similarity of the key parameters controlling modelled precipitation amounts described in section 4.1. Little improvement is obtained repeating the analysis using all 11 RCM members. The differences in the increases in precipitation between each RCM member is likely to be due to natural variability, and/or "noise" in the climate signal.

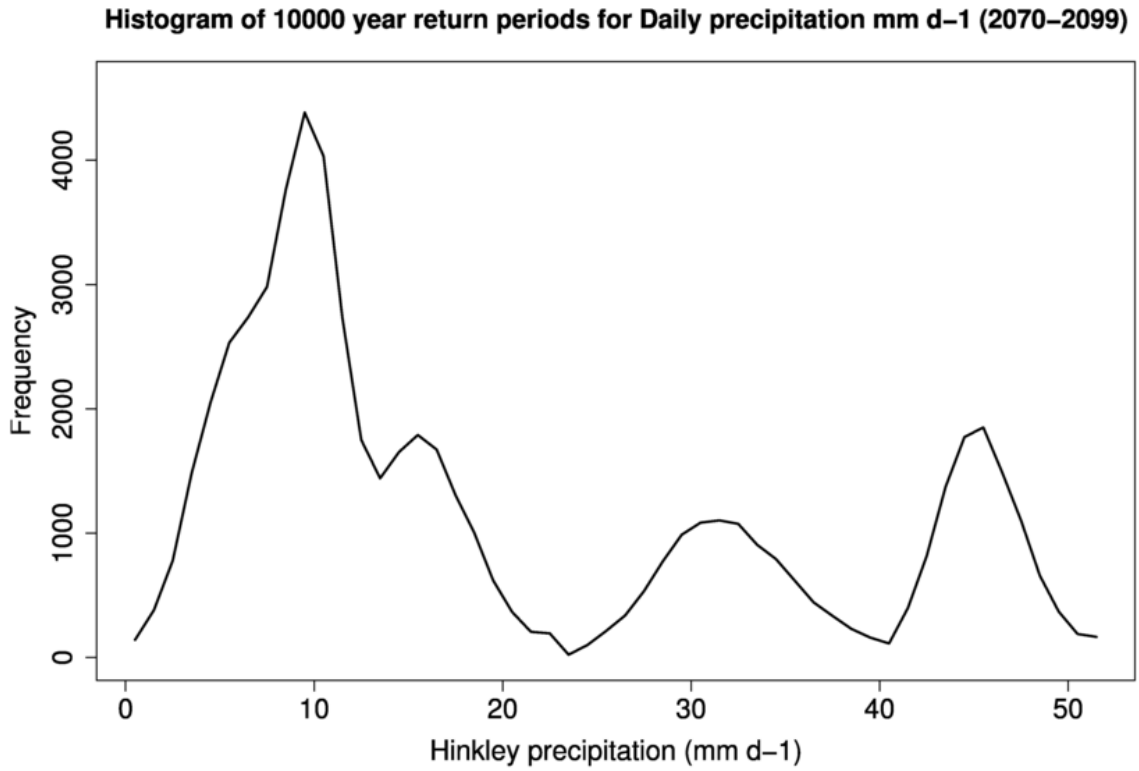

Figure 16. Increase in precipitation for 1 in 10,000 year event, when only the location parameter changes with the covariate. The MPP curves were fitted using the 99.8th percentile to define the extreme values. Results from the 6 preferred RCMs were used to construct the figure.

Two problems are therefore apparent from the initial analysis. First, the location parameter shows little sensitivity to climate change and hence the increase in extreme precipitation is small. Secondly, there are considerable differences between the 6 RCMs studied, despite the fact that they have the same values of the three key parameters identified within the climate model which strongly impacted on modelled precipitation amounts.

The first problem, that of the precipitation sensitivity being rather small, was addressed by repeating the MPP analysis, with the location parameter fixed in time, but instead the

scale parameter was made a function of the covariate. The scale parameter changes the shape of the MPP curve and hence how the extreme rainfall events vary; see Figure 11. An example of the return period amounts (using the 99.8th percentile of the precipitation data to define an extreme event) using this revised approach is shown in Figure 17.

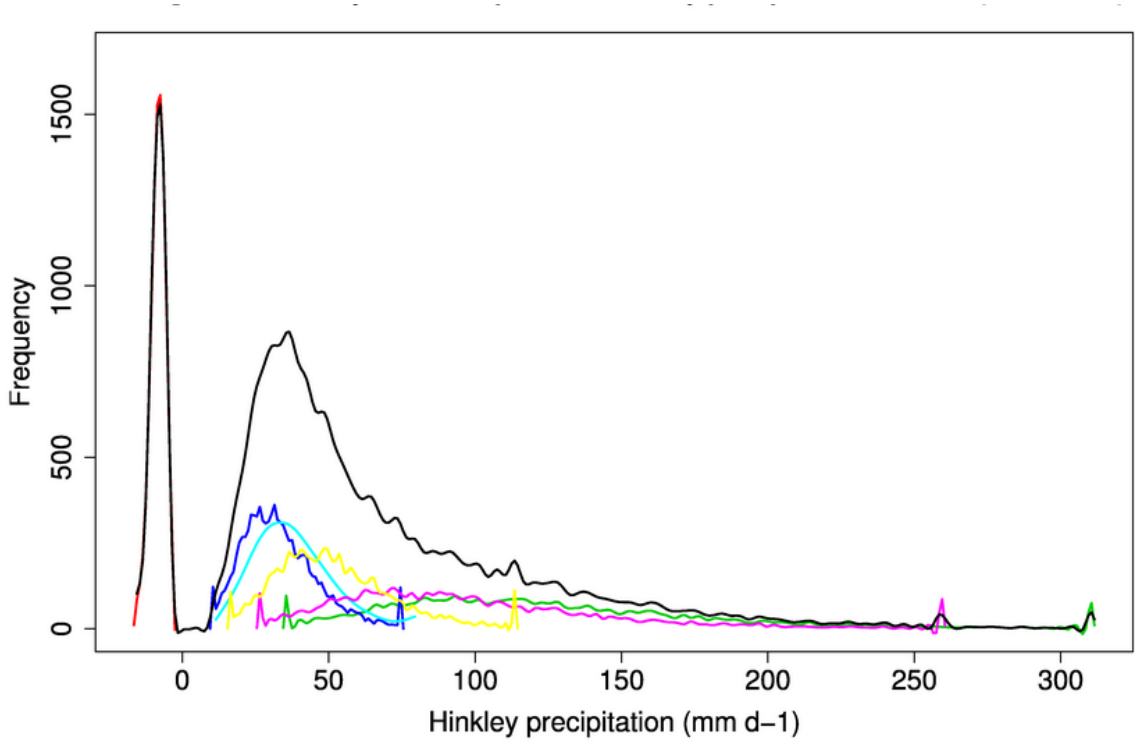

Figure 17. Change in return levels for 1 in 10,000 year precipitation event for the period 2070-2100, when the scale parameter changes with the covariate. The MPP curves were fitted using the 99.8th percentile to define the extreme values. The black line shows the results from combining all 6 models together. Results from each individual RCM are shown by the coloured lines.

Two further tests were made to confirm that this was the best approach. First, the fitting was performed with both the location and scale parameters as functions of the covariate. However the results were essentially the same as when only the scale parameter was allowed to vary. The second test had all three MPP parameters as functions of the covariate, but the fit to the data (using the GOF tests described above) was not improved.

The increase in 1 in 10,000 year precipitation amounts are now much larger (compare Figure 16 with Figure 17). There is still a large spread amongst the models, owing to natural variability and model parameterisation, and one member suggests a small

decrease in extreme precipitation amounts. Some further analysis was performed to investigate the impact of natural variability on the results. Extreme precipitation amounts for the entire UK domain were calculated, using global mean temperature as the covariate. This was used instead of regional temperatures in an effort to reduce any variability caused by regional temperature differences. Additionally, winter and summer rainfall amounts were analysed separately. The extreme events in each of these seasons may change differently with climate change, which could also be contributing to the "noise" in the results.

Results of fitting to the whole period of data (1949-2100) show that sampling uncertainty (manifesting as natural variability) is affecting the derivation of the climate change signal. The spatial patterns of changes in extreme precipitation amounts are not physically plausible. For example, allowing the scale parameter to be non-stationary can produce changes in extremes that have high spatial variability which is greater than would be allowed by the processes affecting extreme rainfall. To minimise this variability, two approaches have been adopted. First, bootstrapping of the input data for the extreme distribution fitting was performed. In this approach, extreme distributions were fitted to multiple samples of half the input data, sampled in 10 year blocks with replacement. 50 bootstraps were used. The MPP parameters obtained from the bootstrapped data were then averaged for each RCM grid box. This averaging reduced the spatial variability to a large degree but did not eliminate it completely. Climate change factors for 1 in 10,000 year extreme precipitation events for every RCM grid box for a global temperature increase of 4 ºC are shown in Figure 18 for all 11 RCM members. This temperature rise was chosen purely for illustrative purposes and does not correspond to a particular emissions scenario. The six preferred RCM members have a solid circle in the upper left hand corner.

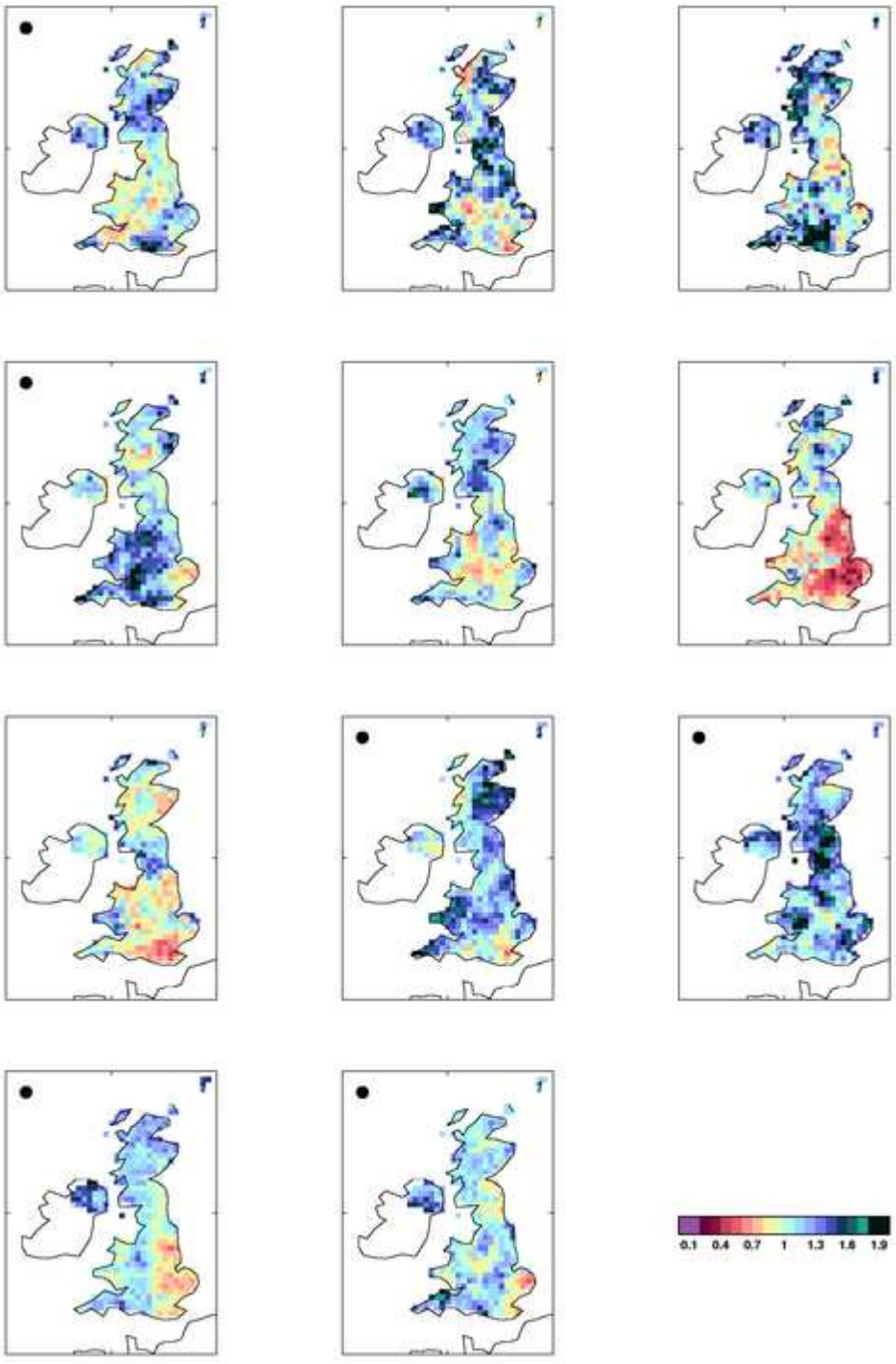

Figure 18. Climate change factors for the end of the 21st century, for 1 in 10,000 year return period rainfall in summer. The six preferred RCM ensemble members are marked by a black circle. These factors were calculated using a global temperature rise of 4 ºC. Despite the efforts to reduce the impact of variability, there are some differences in the climate change factors across the country and between each ensemble member.

These climate change factors are still highly variable across the UK domain, although the variability has been reduced. There are also considerable differences in the climate

change factors between each RCM member. The variability between each of the preferred RCM members is smaller than the entire ensemble, but is still quite large.

The second approach adopted, to further reduce the impact of natural variability, was to average the extreme distribution parameter that expressed the climate change signal (i.e. that which depends on global temperature, here, the scale parameter) over a particular region. For the Hinkley Point application this parameter was averaged for the regions of England and Wales south of The Wash. This area was chosen as a compromise between having a larger area to better average out the sampling uncertainty and a small enough area where the climate change signal can be considered to be quasi-constant. Return levels were calculated using the location and shape parameters for Hinkley Point itself and the averaged scale parameter corresponding to the climate change signal. The covariate was the global mean temperature for each 30 year period used by UKCIP (2010-2039, 2020-2049, ...2070-2099), and the uncertainty was calculated using the probabilistic data from the UKCP09 climate projections (Murphy et al., 2009). The resulting frequency distributions from each RCM member (all 11 were analysed) were combined to create a "best estimate" combined distribution of climate change factors for Hinkley Point for each 30 year period, for summer and winter. Examples of these distributions are shown in Figure 19. It can be seen that there is still considerable difference between the change factors from each of the RCMs (this is especially true for summer) and together form a very poor sample of possible future climate change uncertainty. Overall, all models except 1 project an increase in winter precipitation extremes, whereas there is poorer agreement for summer extremes.

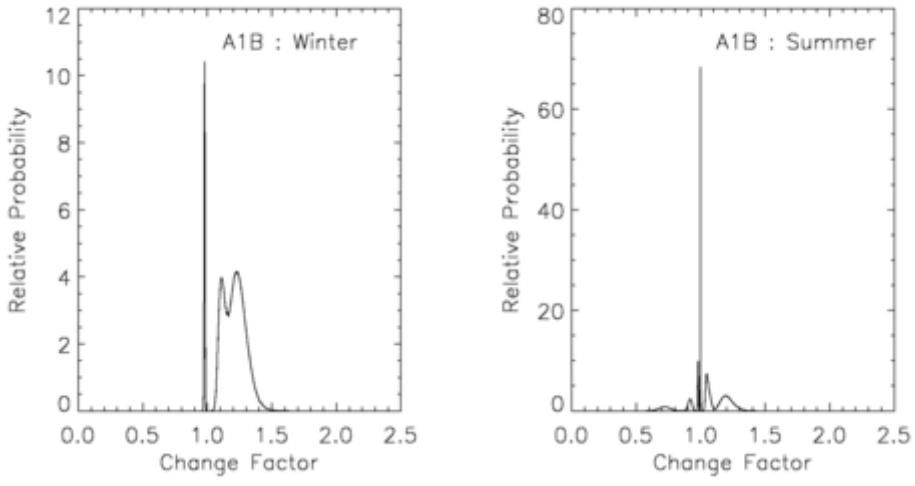

Figure 19. Example of combined distributions using 11 RCM results (A1B Scenario), for 2070-2099 winter and summer for 10,000 year rainfall.

Climate change factors for a range of percentiles were calculated from the combined distribution for each season and 30 year period (i.e. 2010-2039, 2020-2049 ... 2070-2099) for each return period for the A1B emissions scenario. Change factors for 1 in 10,000 year rainfall events are given below in Table 10.

2010-2039		
Percentile	**Winter**	**Summer**
5th	0.99	0.88
25th	1.04	0.99
50th	1.07	1.02
68th	1.09	1.05
75th	1.09	1.06
84th	1.10	1.07
95th	1.12	1.09

2020-2049		
Percentile	**Winter**	**Summer**
5th	0.99	0.85
25th	1.06	0.99
50th	1.09	1.02
68th	1.11	1.07
75th	1.12	1.08
84th	1.13	1.10
95th	1.16	1.12

2030-2059		
Percentile	**Winter**	**Summer**
5th	0.99	0.82
25th	1.07	0.99
50th	1.11	1.03
68th	1.14	1.09
75th	1.15	1.10
84th	1.16	1.12
95th	1.19	1.15

2040-2069		
Percentile	**Winter**	**Summer**
5th	0.98	0.79
25th	1.08	0.99
50th	1.14	1.04
68th	1.17	1.10
75th	1.18	1.12
84th	1.20	1.14
95th	1.23	1.18

2050-2079		
Percentile	**Winter**	**Summer**
5th	0.98	0.77
25th	1.10	0.99
50th	1.16	1.04
68th	1.19	1.12
75th	1.21	1.14
84th	1.23	1.17
95th	1.27	1.21

2060-2089		
Percentile	**Winter**	**Summer**
5th	0.98	0.74
25th	1.11	0.98
50th	1.18	1.05
68th	1.22	1.14
75th	1.24	1.16
84th	1.26	1.19
95th	1.31	1.24

2070-2099		
Percentile	**Winter**	**Summer**
5th	0.98	0.72
25th	1.12	0.98
50th	1.20	1.05
68th	1.24	1.15
75th	1.26	1.18
84th	1.29	1.21
95th	1.34	1.26

Table 10. 10,000 year climate change factors calculated for a range of percentiles, winter and summer, for each 30 year time period to 2099 (A1B scenario).

1 in 100 and 1 in 1,000 year change factors can be found in Table 24 and Table 26 in the Appendix, sections 9.4 and 9.5. These factors must be used with caution, owing to the spread between the individual RCM members, and the very poor sampling of possible future climate change uncertainty.

5. Daily and sub-daily estimates of precipitation at Hinkley Point accounting for climate change

The climate change factors obtained in Section 4 are now applied in this section to the baseline 100, 1,000 and 10,000 year rainfall amounts for Hinkley Point estimated using the FEH (i.e. present day with no climate change element). The results from Sections 2 and 3 indicated that the FEH estimates of rainfall depth for the 10,000 year rainfall return period may be under-estimated based on a comparison with the Cannington/Brymore rain gauge record. After further consideration and consultation of the guidance in Volume 2 (pp. 66) of the FEH (Faulkner, 1999) it is recommended that the baseline rainfall estimates for Hinkley Point used in this study are those obtained from the FEH (sliding duration) for both daily and sub-daily durations.

An additional reason for this recommendation is that the methodology used below to apply the climate change amounts to sub-daily durations relies on the ratio of the daily baseline rainfall to the sub-daily amounts. However there is no rain gauge data available near to the site to assess whether or not the sub-daily estimates should be adjusted, thus it would seem prudent not to adjust the daily rainfall as a result. The baseline rainfall depths for Hinkley Point are presented in Table 11 below.

Return Period/ Duration	Point Rainfall Estimates (mm)		
	15-minute	1-hour	Daily
1 in 100 years	33.3	44.6	92.6
1 in 1,000 years	69.5	85.5	145.6
1 in 10,000 years	145.1	163.7	228.8

Table 11. FEH Rainfall return period estimates for Hinkley Point (obtained using AMAX records, at a point location for a sliding duration). These are the baseline estimates to which the climate change factors will be applied.

5.1 Adjustment of baseline rainfall to account for climate change

The factors calculated in Section 4 can be applied directly to the baseline daily rainfall estimates in Table 11 using Equation 12 because the RCM rainfall output is calculated on a daily duration. However, these factors cannot be directly applied to the sub-daily durations. Therefore the growth factor (i.e. the ratio) between each sub-daily estimate

and the daily estimate at each return period has been calculated (Table 12) and used to scale the climate change estimates for the daily duration to a more realistic estimate of sub-daily rainfall using Equation 13.

Equation 12

Daily Rainfall Depth (mm) = change factor × baseline daily rainfall

Equation 13

Sub-daily Rainfall Depth (mm) = ([(change factor – 1) × ratio] + 1) × baseline rainfall

Return Period/Duration	Growth Factor/Ratio	
	15-minute	1-hour
1 in 100 years	0.360	0.482
1 in 1,000 years	0.477	0.587
1 in 10,000 years	0.634	0.715

Table 12. Calculated growth factors between daily and sub-daily rainfall estimates obtained from FEH at different return periods.

It may be assumed that the ratios given in Table 12 may vary in the future with climate change. Indeed, Lenderick and Van Meijgaard (2008) suggest that hourly extreme rainfall is likely to increase more than daily extremes in large parts of Europe. However research in this field is very limited, thus, for the purposes of this study the ratios are assumed to remain constant.

The results of applying the equations above produce estimates of extreme rainfall depths at Hinkley Point at the three different durations for each season (winter and summer) and each 30 year time period, from 2010-2039 to 2070-2099. The results for the 10,000 year rainfall are presented below in Section 5.2, Table 13. The results for 100 and 1,000 year rainfall depths can be found in the Appendix, Section 9.4 Table 24 and Section 9.5 Table 26 respectively.

5.2 Extreme rainfall estimates for Hinkley Point accounting for climate change

The adjusted rainfall estimates for 10,000 year winter and summer rainfall throughout the 21st century are shown in Table 13 and an example of the resulting rainfall growth curves can be seen in Figure 20. Tables for the 100 and 1,000 year estimates can be found in the Appendix, sections 9.4 and 9.5 respectively. The summary data enables

EDF and the NII to reach mutual agreement on a figure that is most appropriate for drainage design at the site, not just in terms of rainfall depth, but also through consideration of estimated design life of the project (approximately 60 years).

2010-2039: Winter				
%ile	Change Factor	15 minute	1 hour	1 day
5th	0.99	144.3	162.7	226.8
25th	1.04	149.2	168.9	238.9
50th	1.07	151.6	172.0	244.9
68th	1.09	153.0	173.8	248.5
75th	1.09	153.6	174.5	249.9
84th	1.10	154.5	175.6	252.1
95th	1.12	156.1	177.8	256.3

2010-2039:Summer				
%ile	Change Factor	15 minute	1 hour	1 day
5th	0.88	134.5	150.2	202.5
25th	0.99	144.5	162.9	227.3
50th	1.02	146.9	166.0	233.2
68th	1.05	150.0	169.9	240.9
75th	1.06	150.9	171.1	243.3
84th	1.07	151.9	172.4	245.7
95th	1.09	153.5	174.4	249.7

2020-2049: Winter				
%ile	Change Factor	15 minute	1 hour	1 day
5th	0.99	144.1	162.4	226.3
25th	1.06	150.4	170.4	241.9
50th	1.09	153.6	174.5	249.8
68th	1.11	155.4	176.8	254.4
75th	1.12	156.1	177.8	256.2
84th	1.13	157.3	179.2	259.1
95th	1.16	159.5	182.0	264.5

2020-2049:Summer				
%ile	Change Factor	15 minute	1 hour	1 day
5th	0.85	131.7	146.6	195.5
25th	0.99	144.3	162.7	226.9
50th	1.02	147.4	166.6	234.5
68th	1.07	151.5	171.8	244.7
75th	1.08	152.7	173.4	247.7
84th	1.10	154.0	175.0	250.9
95th	1.12	156.1	177.6	256.0

2030-2059: Winter				
%ile	Change Factor	15 minute	1 hour	1 day
5th	0.99	143.9	162.1	225.7
25th	1.07	151.6	172.0	244.9
50th	1.11	155.6	177.1	255.0
68th	1.14	157.9	180.0	260.6
75th	1.15	158.8	181.1	262.9
84th	1.16	160.2	182.9	266.4
95th	1.19	162.9	186.4	273.1

2030-2059:Summer				
%ile	Change Factor	15 minute	1 hour	1 day
5th	0.82	128.9	143.1	188.6
25th	0.99	144.1	162.5	226.4
50th	1.03	147.9	167.3	235.9
68th	1.09	153.1	173.9	248.7
75th	1.10	154.6	175.7	252.3
84th	1.12	156.1	177.7	256.2
95th	1.15	158.7	181.0	262.6

2040-2069: Winter				
%ile	Change Factor	15 minute	1 hour	1 day
5th	0.98	143.7	161.9	225.2
25th	1.08	152.8	173.6	248.1
50th	1.14	157.7	179.8	260.2
68th	1.17	160.5	183.3	267.0
75th	1.18	161.6	184.7	269.8
84th	1.20	163.3	186.8	274.0
95th	1.23	166.6	191.0	282.2

2040-2069:Summer				
%ile	Change Factor	15 minute	1 hour	1 day
5th	0.79	126.2	139.6	181.8
25th	0.99	144.0	162.2	226.0
50th	1.04	148.5	168.0	237.2
68th	1.10	154.7	176.0	252.7
75th	1.12	156.5	178.2	257.1
84th	1.14	158.4	180.6	261.8
95th	1.18	161.5	184.6	269.6

Table 13. 1 in 10,000 year rainfall estimates (in mm) for durations of 15 minutes, 1 hour and 1 day at Hinkley Point by season for 2010-2039, 2020-2049, 2030-2059 and 2040-2069 for a range of percentiles.

2050-2079: Winter				
%ile	Change Factor	15 minute	1 hour	1 day
5th	0.98	143.5	161.6	224.7
25th	1.10	154.0	175.0	251.0
50th	1.16	159.7	182.3	265.1
68th	1.19	162.9	186.4	273.1
75th	1.21	164.2	188.0	276.3
84th	1.23	166.2	190.6	281.3
95th	1.27	170.1	195.5	290.9

2050-2079:Summer				
%ile	Change Factor	15 minute	1 hour	1 day
5th	0.77	123.8	136.6	175.8
25th	0.99	143.8	162.0	225.5
50th	1.04	149.0	168.7	238.5
68th	1.12	156.2	177.9	256.5
75th	1.14	158.3	180.5	261.6
84th	1.17	160.5	183.3	267.0
95th	1.21	164.2	188.0	276.2

2060-2089: Winter				
%ile	Change Factor	15 minute	1 hour	1 day
5th	0.98	143.3	161.4	224.3
25th	1.11	155.1	176.5	253.8
50th	1.18	161.6	184.7	269.8
68th	1.22	165.3	189.4	279.0
75th	1.24	166.8	191.3	282.7
84th	1.26	169.1	194.2	288.5
95th	1.31	173.6	200.0	299.8

2060-2089:Summer				
%ile	Change Factor	15 minute	1 hour	1 day
5th	0.74	121.6	133.7	170.3
25th	0.98	143.6	161.8	225.2
50th	1.05	149.5	169.3	239.8
68th	1.14	157.7	179.7	260.0
75th	1.16	160.0	182.7	265.9
84th	1.19	162.6	185.9	272.2
95th	1.24	166.9	191.4	282.9

2070-2099: Winter				
%ile	Change Factor	15 minute	1 hour	1 day
5th	0.98	143.1	161.2	223.9
25th	1.12	156.1	177.7	256.2
50th	1.20	163.3	186.8	274.0
68th	1.24	167.4	192.1	284.2
75th	1.26	169.0	194.2	288.3
84th	1.29	171.7	197.5	294.8
95th	1.34	176.8	204.0	307.5

2070-2099:Summer				
%ile	Change Factor	15 minute	1 hour	1 day
5th	0.72	119.6	131.3	165.5
25th	0.98	143.5	161.7	224.8
50th	1.05	149.9	169.9	240.8
68th	1.15	158.9	181.3	263.2
75th	1.18	161.5	184.6	269.7
84th	1.21	164.4	188.3	276.8
95th	1.26	169.2	194.4	288.7

Table 13 (continued). 1 in 10,000 year rainfall estimates (in mm) for durations of 15 minutes, 1 hour and 1 day at Hinkley Point by season for 2050-2079, 2060-2089 and 2070-2099 for a range of percentiles.

It must be remembered that the 11 sets of RCM results poorly sample the “true” distribution of changes in extreme precipitation (hence the multiple peaks in the combined distribution shown in Figure 19). Hence the climate change factors and 1 in 100, 1,000 and 10,000 year precipitation amounts must be used with caution.

A summary of the range of 10,000 year rainfall depths projected out to 2099 for each rainfall duration period is presented in Table 14. In comparison with the baseline estimates (Table 11), there is the potential for a very slight decrease in rainfall in winter (to a maximum of 4.9 mm) as opposed to projected increases of 31.7, 40.0, and 78.7 mm for 15-minute, hourly and daily durations respectively. The increases projected in summer are not as large (24.1, 30.7 and 60.0 mm) though the projected drop in precipitation extends to a maximum of 63.3 mm for daily rainfall.

Duration	Winter	Summer
	Range of estimates (mm)	Range of estimates (mm)
15 minutes	143.1 – 176.8	119.6 – 169.2
1 hour	161.2 – 204.0	131.3 – 194.4
1 day	223.9 – 307.5	165.5 – 288.7

Table 14. Range of 10,000 year rainfall estimates accounting for climate change to 2099.

There are few key points to note from Table 13 and Table 14 some of which can be identified by examining Figure 20, which shows the change factors applied to the 10,000 year baseline estimates for each 30 year time period, winter and summer.

A. Winter rainfall is consistently projected to be greater compared to the equivalent percentile and duration in summer rainfall.
B. The largest precipitation estimate is found under the winter 2070-2099 projections for the 95th percentile.
C. Values in winter and summer, at the 50th percentile and above, all project an increase in precipitation for all durations.
D. The change factors calculated for both winter and summer, out to 2099 from the 5th percentile, consistently project a decrease in precipitation. It is also the case that there are some reductions at the 25th percentile as well.
E. The range in projected rainfall amounts in both winter and summer increases with time.

Summary tables for the adjusted rainfall amounts for 100 and 1,000 year rainfall return periods can be found in the Appendix, section 9.4 (Table 25) and section 9.5 (Table 27) respectively. The same points detailed above can be attributed to the 100 and 1,000 year rainfalls with the exception of point D. In general the change factors calculated at the 5th percentile predict a decrease, though there are some exceptions in the 100 year results, where the change factor is either equal to 1.00, indicating no change, or 1.01, a very slight increase.

It should be noted that the methodology used to derive the rainfall estimates has applied seasonal change factors to baseline estimates calculated using an annual time series (the annual maximum (AMAX)). Ideally seasonal baseline estimates would have been calculated at Hinkley Point, but this would only have been feasible for daily rainfalls, as

there are no sub-daily rainfall observations available. Therefore the use of the FEH is most appropriate. A further alternative would be to calculate the climate change factors annually, effectively the average between winter and summer, and apply this to the annual baseline estimates. However, given that the HadRM3 model cannot accurately resolve summer convection, but that winter frontal rainfall is well represented, a model that could resolve convection may be expected to produce climate change factors in excess of the winter factors calculated in this study, thus increasing the final winter rainfall estimates produced in Table 13. Therefore, as these estimates are being applied for the design of drainage to protect critical infrastructure, the approach adopted is the most resilient.

The greatest confidence is placed in the 1 in 100 year rainfall estimates, as this return period is closest to the length of the available precipitation record. The uncertainty in the return level increases with longer return periods as is discussed in the Appendix, Section 9.1 and is illustrated in Figure 11. Similarly, the uncertainty in the climate change factors also increases with longer return periods, as the climate change factors are calculated by dividing the future return level by the present day return level. This should be considered when selecting an appropriate design rainfall for drainage design.

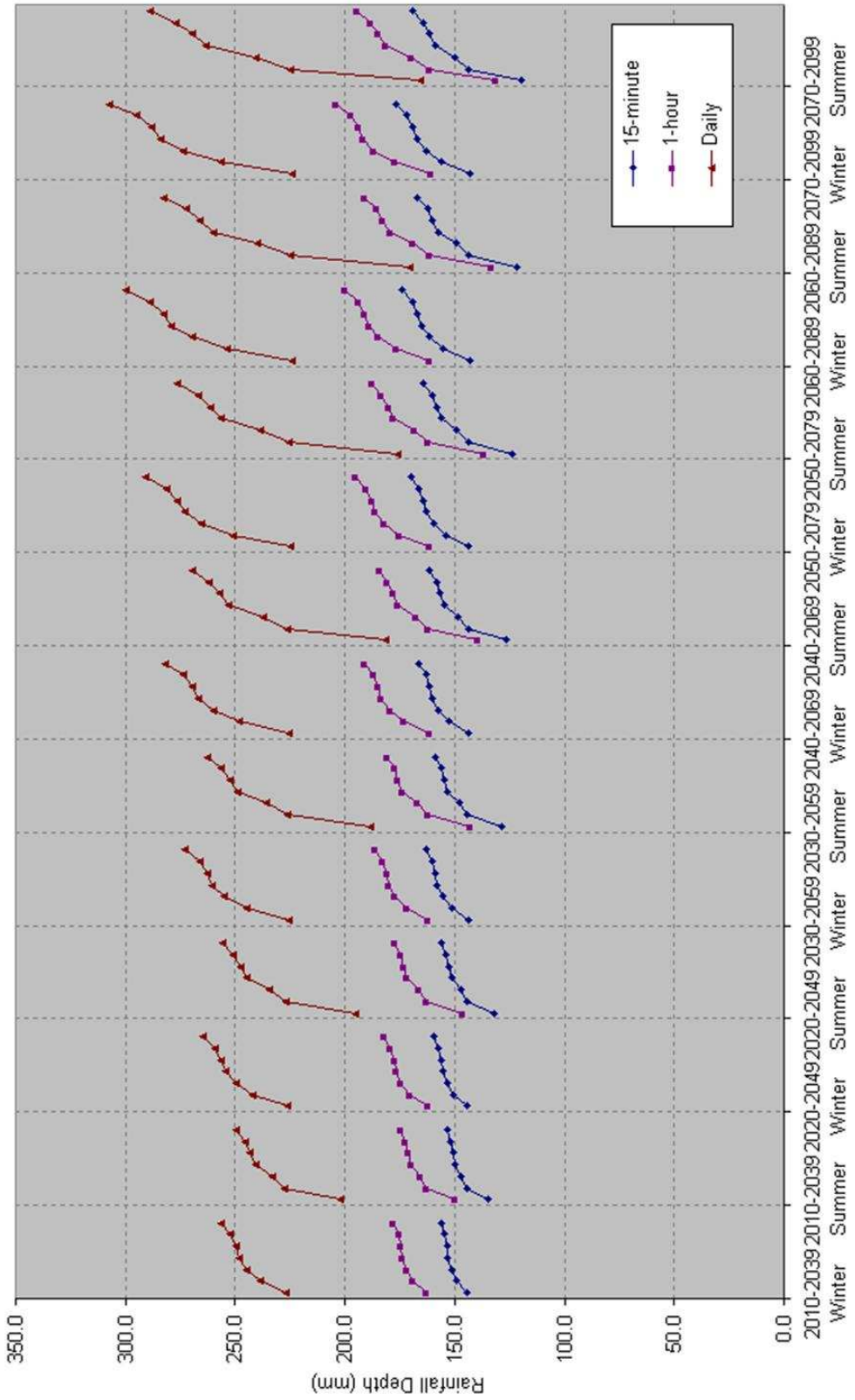

Figure 20. Summary of 10,000 year precipitation projections at the seven percentiles out to 2099. The seven points on each line indicate the rainfall depths for (starting at the bottom) the 5th, 25th, 50th, 68th, 75th, 84th and 95th percentiles respectively.

6. Estimation of Probable Maximum Precipitation at Hinkley Point

Probable Maximum Precipitation (PMP) is a concept widely used in engineering design where the failure of a structure or system is considered to have severe consequences. PMP is a rationalised estimate of the upper limit of precipitation for a given duration and location, and is based on physical consideration of the structure of the atmosphere and rain producing systems, in combination with statistics (Lewis, 1991). Both the physical and statistical approaches are aimed at producing an estimate with a very long return period. The return period associated with PMP is not rigidly defined, but is considered to be in the order of 10^5 or greater (US Corps of Engineers, 1997). It thus provides a check against the rainfall estimates of extreme rainfall, particularly the 10,000 year estimates, accounting for climate change produced in this study.

In this examination, estimates of PMP have been derived from 3 methods:

1. World Meteorological Organisation (WMO) method (WMO, 1986)
2. Flood Studies Report (FSR) method (NERC, 1975)
3. Rapid statistical method (WMO, 2009)

Interestingly for this study, there is the information available for the Cannington-Brymore storm of 18th-19th August, 1924. This event is widely recognised as one of the 5 most severe events ever recorded in England.

6.1 Calculations of Probable Maximum Precipitation

6.1.1 WMO Method

The WMO method of estimating PMP is an international standard, fully documented in the Manual, WMO No. 332, (WMO, 1986). The basis of the method can be expressed in the formula shown in Equation 14,

Equation 14

$$M = \frac{R.W_{100}}{W_s}$$

where M is the maximised area or point rainfall and R is the observed area or point rainfall amount. W_{100} is the precipitable water estimated from the dew point temperature with a 100-year return period for the month concerned, and W_s is the precipitable water estimated from a representative dew point for the observed storm. $T_{dew}(100)$ and T_{dew} will refer to the dew point temperature with a 100-year return period and representative dew point for the storm respectively.

The largest observed storm is that of August 1924, which as has already been noted, exceeds the estimate of the 10,000 year rainfall, and approximates to current best-estimates of PMP. There are reservations about the justification of applying maximising multipliers to this event. The summary depth-duration information for this storm, as taken from the British Rainfall report (Glasspoole, 1924), are summarised in Table 15.

Duration (hours)	Depth (mm)
2	127.0
5	203.0
8	238.8

Table 15. Depth-Duration data for Cannington-Brymore storm, August 1924.

The FSR chapter on "Estimated maximum falls of rain" (NERC, 1975, Ch.4) gives an estimated dew point temperature (T_{dew}) for the storm of 15 ^{o}C. This value would appear to be too low, and its provenance, such as time of day of reading, upper atmosphere structure, etc., cannot be checked at this distance in time. Analysis of dew point data from the Met Office weather station at Yeovilton for August gives a mean annual maximum dew point temperature of 17.9 ^{o}C. Given that a large storm could equally occur in July, when temperatures are higher than August (such as the severe storm of July 1968 which affected the nearby Mendip Hills), estimation of $T_{dew}(100)$ has been carried out by a probability analysis of the annual maximum series of T_{dew} in July and August from the closest Met Office observation stations, at Yeovilton, Somerset and Rhoose, near Cardiff. The results are illustrated in Figure 21 and summarised in Table 16.

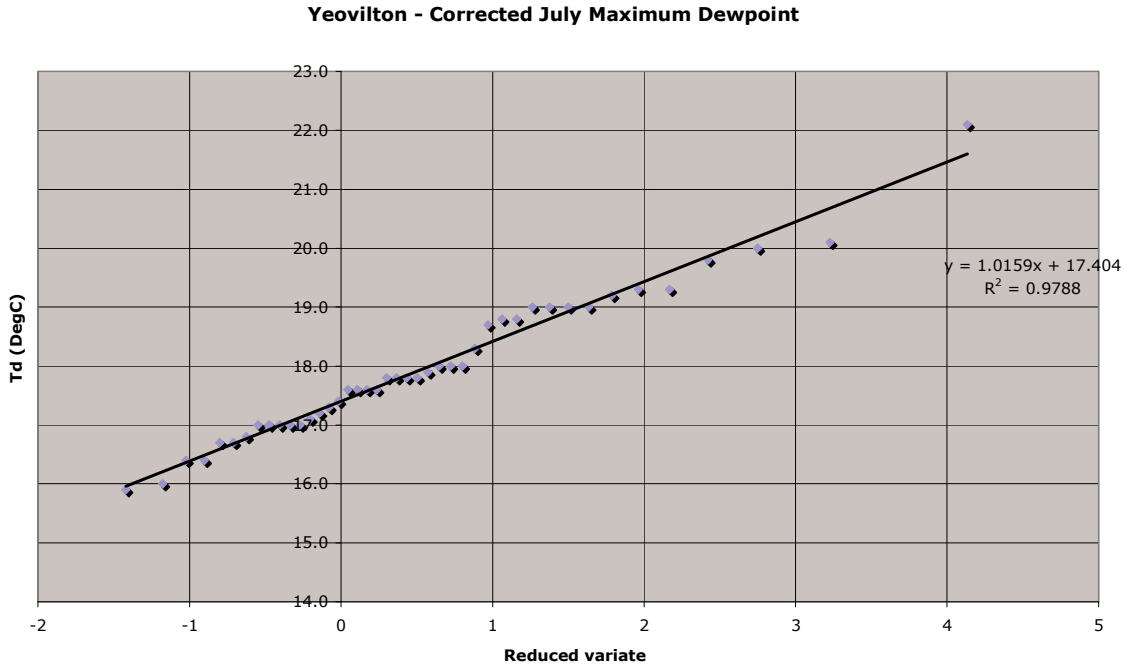

a) T_{dew} series for Yeovilton, July, omitting 2 anomalous values

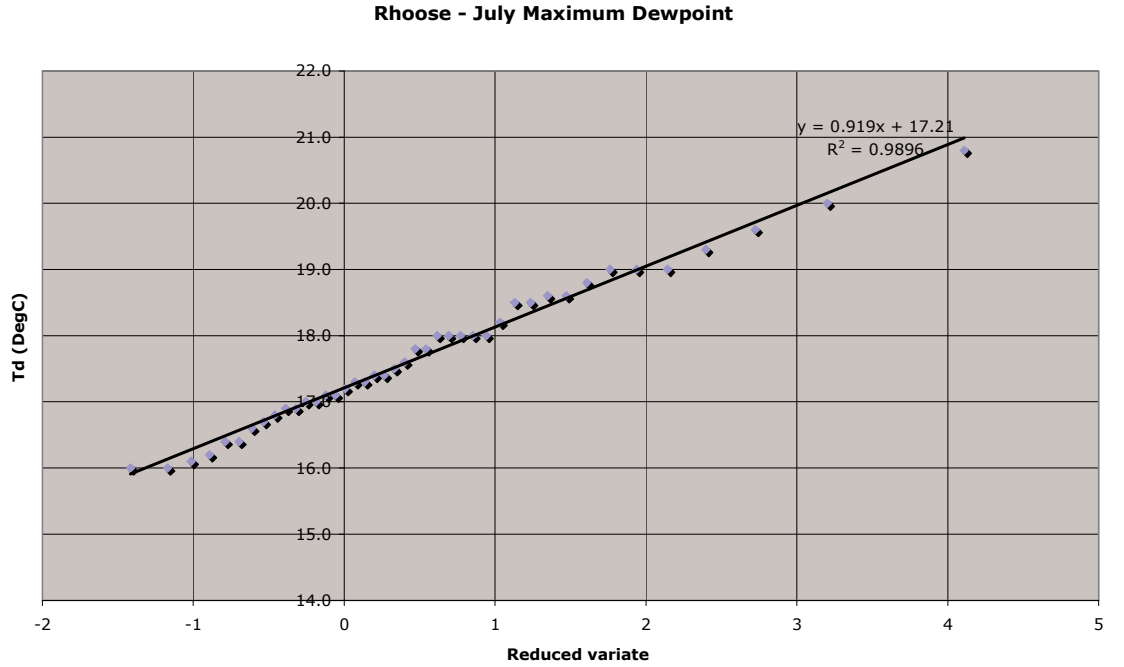

b) T_{dew} series for Rhoose, July, all data

Figure 21. Examples of T_{dew} annual maximum probability plots (the Gumbel reduced variate is used here to estimate the return period of an event)

Station	Month	$T_{dew}(100)$ (°C)	W_{100} (mm)	Max'n Ratio
Yeovilton	July	22.1 (24.8*)	63.5	1.92
	August	21.4	59	1.79
Rhoose	July	21.4	59	1.79
	August	20.7	55	1.67

Table 16. Estimates of $T_{dew}(100)$, W_{100} and maximisation ratio for representative stations. (*This higher estimate is the result of bias introduced by two anomalous high readings, which have been omitted to provide the best fit relationship).

The maximisation ratio (MR) may be calculated as follows:

For $T_{dew}(mean) = 17.9\ ^{o}C$, $W_{mean} = 43mm$

For $T_{dew}(100) = 22.1\ ^{o}C$, $W_{100} = 63.5mm$

So $MR = W_{100} / W_{mean} = 63.5 / 43 = \underline{1.476}$

As the location of Hinkley Point and the observation stations are close to sea level, no adjustment is required for orographic influence. Applying the maximisation ratio to the observed rainfalls in Table 15, the estimates of PMP obtained are summarised in Table 17.

Duration / hours	PMP depth (mm)	MR Reduction factor	PMP adjusted (mm)
2	187	1.0	187
5	300	0.96	288
8	352	0.92	324

Table 17. Estimates of PMP for different durations, using the WMO method. See text for description of calculation of MR reduction factors.

It should be noted that the estimate of $T_{dew}(100)$ is made from annual maximum 1-hour values of T_{dew}. The maximisation ratio should reflect the duration of the storm event. The WMO method recommends the use of 6-hour or 12-hour persistent T_{dew} values, i.e. the average of T_{dew} over those periods. Examination of persistence of dew point temperatures from a few representative records from Met Office stations at Yeovilton, Dunkerswell and Boscombe Down suggest that the maximisation ratio may be reduced by factors of 0.96 for a 6-hour duration, 0.91 for a 12-hour duration and 0.88 for a 24-

hour period. These values are applied in the “PMP adjusted” column in Table 17, with a factor of 0.96 being applied to the 5-hour duration and 0.92 to the 8-hour duration.

As the maximum recorded rainfall of 238.8 mm at Cannington/Brymore is also treated as a 1-day value for the AMAX exceedance series, it is assumed that the 8-hour value of 352 mm can also be applied to the 1-day value. The adjusted PMP figure for a 24-hour rainfall is given by the following calculation:

PMP adjusted = 352 x 0.88 = 310 mm

6.1.2 FSR Method

The FSR method, which has not been changed by later editions of FEH, is similar to the WMO method, in that it is based on estimates of precipitable water. The process of calculation is made using graphs and tables in Chapter 4 of FSR Vol II (NERC, 1975). The starting point is the 1 in 5 year estimate of precipitable water (M5-6hr), based on 6-hour persistent dew point temperature. This statistic for the UK is presented as a map of iso-lines in Figure 3.8 of FSR, Vol II (NERC, 1975). The 1 in 5 year precipitable water for the Hinkley Point locality is 46 mm, and the map shows that Hinkley Pont lies in one of the areas of highest precipitable water for the UK.

FSR suggests that the maximum value of precipitable water is 20-25% greater than the M5 value: thus conservatively, the maximum precipitable water (P_w(max)) can be calculated using the following:

P_w(max) = 46 x 1.25 = 57.5 mm

This value is similar to the estimates from the T_{dew}(100) analyses, shown in Table 16 above, which range from 55 to 63.5 mm.

FSR bases maximisation on “storm efficiency”, which was obtained by analysing a number of major historic storms in the UK, including the Cannington/Brymore storm of 1924 (Glasspoole, 1924). FSR recommends the multiplying of P_w(max) value by a factor of 3.86 to estimate the 2-hour PMP. Thus the 2-hour PMP value for the Hinkley Point site is:

57.5 x 3.86 = 222 mm

FSR is not clear on the method to estimate PMP for other durations, but suggests various multipliers of average annual rainfall (AAR) and the 1 in 5 (M5) 2 day rainfall estimates. Multipliers are provided in generalised tables (Table 4.1 and 4.2 of FSR Vol. II (NERC, 1975), giving the following estimates:

15-minute PMP = 0.47 x 222 = 104 mm

60-minute PMP = 0.83 x 222 = 185mm

24-hour PMP = 285 mm

When the four values for PMP from the FSR method are plotted on a semi-logarithmic scale (Figure 22), a reasonable straight-line fit is obtained, although some curvature is evident. Using the estimating equation, shown as the equation of the best fit line in Figure 22 below, values for the 5 and 8 hour PMP can be obtained for comparison with the recorded values for the Cannington-Brymore storm (Table 18).

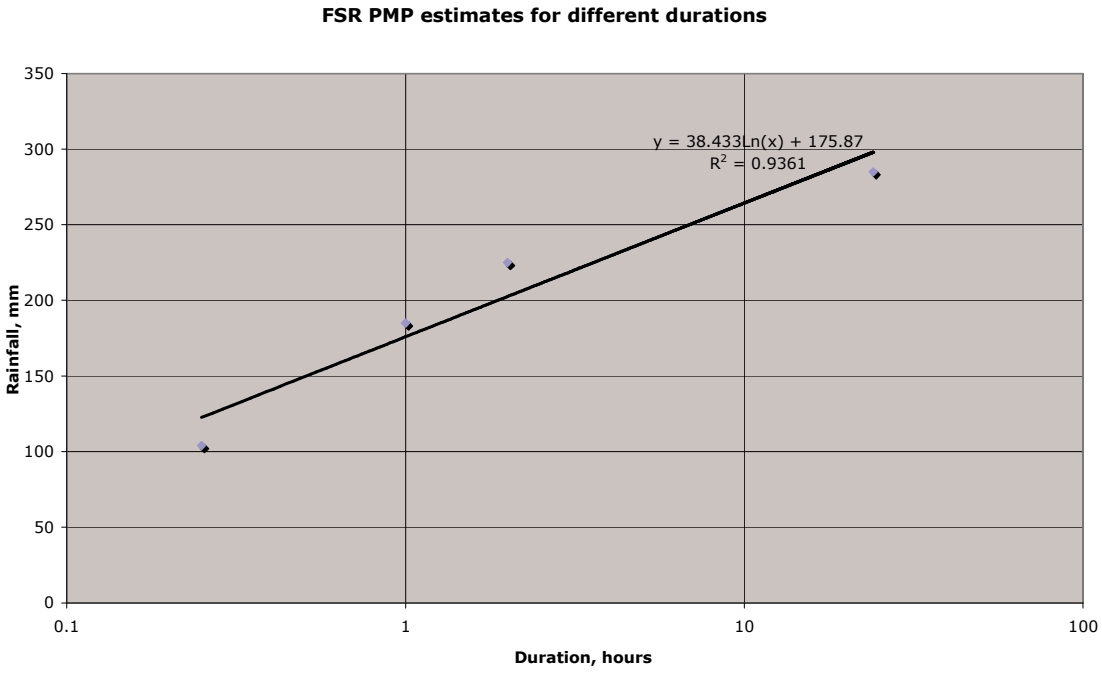

Figure 22. Estimates of PMP for different durations, from FSR. The PMP values are shown on the y-axis.

Duration (hours)	FSR-PMP estimate (mm)	Cannington-Brymore storm measurements (mm)
5	238.0	203.0
8	256.0	238.8

Table 18. Comparison of FSR-PMP estimates with recorded maximum rainfall (mm).

6.1.3 Rapid statistical method

The Herschfield Method, described in the WMO Guide to Hydrological Practices (WMO, 1994; WMO, 2009) is a general statistical method, which is useful to check the validity of other estimates of PMP. It is specifically intended to be used to estimate PMP for point locations or small areas, and uses long-term annual maximum data. The estimation of PMP by this method is given by Equation 15,

Equation 15

$$PMP = P_{mean} + K.S_p$$

where K is a factor dependent on the magnitude of P_{mean} and duration, and S_p is the standard deviation of the annual maximum series. It is recommended that if an annual maximum series contains one or more outliers, they should be excluded from the calculation of mean and standard deviation. The Herschfield Method has been applied to the annual maximum daily series for Cannington-Brymore, in which the 1924 storm value has been excluded, and for Whitewick, where the complete series can be used, as it contains no outliers. The results are remarkably similar, as shown in Table 19.

Location	1-day Mean (mm)	Standard deviation (mm)	K value	24-hour Mean* (mm)	24-hour PMP (mm)
Cannington-Brymore	37.2	16.17	18	43	334
Whitewick Farm	36.6	16.63	18	42.5	342

Table 19. Estimates of 24-hour PMP by Herschfield Method

* 1-day value converted to 24-hour value by a factor of 1.16, as recommended by WMO, 2009. Storm totals therefore accumulated for any start time in a 24-hour period. This reflects reality more closely as storm events may traverse the fixed measuring periods (i.e 09-09 GMT) used at gauging sites (1-day value).

As there are no observed 1-hour rainfall values from which an annual maximum series can be calculated, an approximation of the 1-hour PMP can only be estimated by using the generalised relationship between the values of K for 1 hour and 24 hours in Figure 29.3 of the WMO Guides (WMO, 1994; WMO, 2009). Using the 24-hour rainfall values, the K value for 1 hour is 11, i.e. 0.62 of the 24-hour value. Applying his factor to the PMP estimates in Table 19 gives a 1-hour PMP estimate of 210 mm (the application of this factor is shown graphically in Figure 23). The straight line connecting these points can be extrapolated downwards to 15 minutes using Equation 16, where the duration (x) is in hours, and so x = 0.25 for a 15 minute period.

Equation 16

$$PMP = 40.276.\ln(x) + 210$$

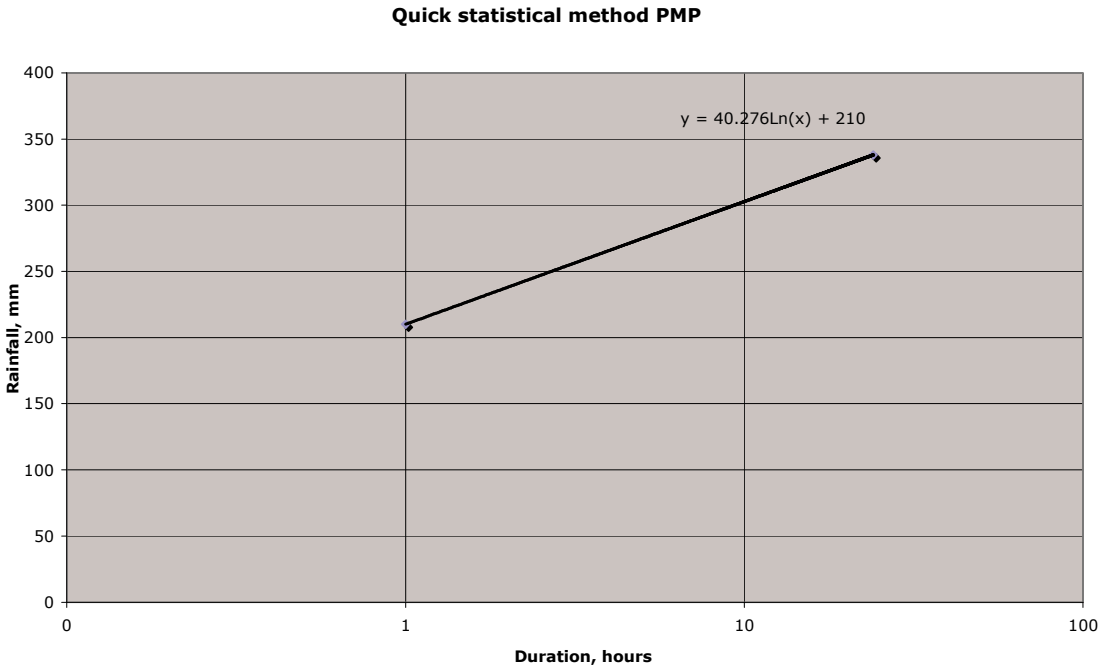

Figure 23. Relationship between 24-hour and 1-hour rainfall from WMO Guides (WMO, 1994; WMO, 2009). The 15 minute PMP value is calculated from the 1 hour value using Equation 16.

The application of Equation 16 provides an estimate for the 15-minute PMP of 154 mm.

6.2 Summary of Probable Maximum Precipitation results

The three methods used in sections 6.1.1-6.1.3 to calculate PMP cannot be used in a way that all can produce consistent direct estimates of PMP at the specified time intervals (15 minutes, 1 hour and 1 day). Some methods use data, and others generalised factors. Given this, the range of estimates produced using the three methods are summarised in Table 20, column 2.

Duration	Range of PMP estimates (mm)	10,000 year winter estimates (mm)
15 minutes	104 – 154	143.1 – 176.8
1 hour	185 – 210	161.2 – 204.0
1 day	285 – 310	223.9 – 307.5

Table 20. Range of PMP estimates and as a comparison, the range of 10,000 year winter rainfall estimates accounting for climate change (taken from Table 13, Section 5.2).

Table 20 suggests that the range of 10,000 year rainfall estimates accounting for climate change (winter estimates) is acceptable as the results are not significantly different from the PMP estimates. It would be of concern if the rainfall estimates were greatly in excess of the estimated physical upper limits of precipitable water at Hinkley Point. It is of interest that the 10,000 year 15-minute baseline rainfall estimate from the FEH (145.1mm) falls within the range of the 15-minute PMP even before the climate change factors have been applied. As such, after applying the climate change factors for winter the estimated maximum rainfall is in excess of PMP. This is probably due to applying the FEH beyond its recommended application (i.e. at durations of less than 30 minutes), as discussed in the Appendix. However, with no rain gauges close to the site recording sub-daily rainfall totals, this is the best approximation of rainfall at the site for this duration.

6.3 Climate Change and Probable Maximum Precipitation

The postulated future under various climate change scenarios gives a range of higher temperatures. This therefore implies that a warmer atmosphere will be capable of holding more moisture, and also implies greater thermo-dynamic activity. Thus dew point temperature (T_{dew}) may be expected to rise in some manner closely correlated with a rise in temperature (T). This will result in an increase in precipitable water (W). Using an

increased estimate for $T_{dew}(100)$ will therefore increase the maximisation ratio W_{100}/W_s, as given in Equation 14.

The WMO Manual (WMO, 1986) on the estimation of PMP does not include any guidance on making allowance for climate change. A new edition of the Manual is currently being finalised, and it may be worth revisiting the topic of PMP should revisions suggest it.

7. Summary and Recommendations

1 in 100, 1,000 and 10,000 year rainfall amounts for winter and summer have been estimated for Hinkley Point using a combination of statistical manipulation of observed data and modelled rainfall amounts. Modelled daily precipitation amounts from an 11 member regional climate model ensemble (A1B emission scenario), which were released alongside the UKCP09 climate projections, have been analysed using extreme value analysis (EVA). In this approach, a distribution defined by three parameters (called location, scale and shape) is fitted to the extreme precipitation data. One or more of the parameters may vary with climate.

Three different approaches were tried. The first, which effectively assumed a linear increase in extreme precipitation with temperature (i.e., the location parameter only was assumed to be a function of temperature) produced only a small increase, somewhat smaller than might be expected. The second approach, where the shape of the distribution was allowed to change with temperature produced much larger precipitation changes. However, there was little coherence in the climate change signals on expected spatial scales and consistency between individual RCM ensemble members was poor. Winter and summer rainfall amounts were not separated.

Natural variability in and between each member was found to be large, and was causing significant uncertainty in determining the extreme distributions. Efforts were made to reduce this uncertainty to an acceptable level, from which distributions of climate change factors could be calculated. Extreme value analysis was performed for all land points within the UK, treating winter and summer rainfall separately. It was found that natural variability was affecting the derivation of the climate change signal as spatial patterns of changes in extreme precipitation amounts were not physically plausible. To minimise the effects of natural variability, the Met Office have adopted a third approach. Extreme value distributions were fitted to multiple samples of the input data, which were sampled in 10 year blocks with replacement (a process known as bootstrapping). The sampled extreme value parameters were then averaged for each grid box which reduced the spatial variability to a large degree but not completely. Next, the extreme distribution parameter that expressed the climate change signal (i.e. that which depends on global temperature) was averaged over a large area. Here, only the scale parameter is

assumed to change with global mean temperature. For the Hinkley Point application this parameter was averaged for the regions of England and Wales south of The Wash.

All models bar one predict an increase in extreme rainfall in winter. Changes in extreme summer rainfall amounts are much less certain, as several models project a decrease, whereas the remainder suggest an increase. These climate change factors were applied to the baseline 100, 1,000 and 10,000 year rainfall amounts calculated using the FEH to produce the final rainfall estimates for EDF and the NII to consider in the context of drainage design and flood risk.

The greatest confidence is placed in the 1 in 100 year rainfall estimates, as this return period is closest to the length of the available precipitation record. The uncertainty in the return level increases with longer return periods. In the same way, the uncertainty in the climate change factors increases with longer return periods, as the factors are calculated by dividing the future return level by the present day return level. The calculation of PMP using three methods at Hinkley Point was an attempt to place an upper physical limit on precipitation. The 10,000 year rainfall estimates accounting for climate change fall within the range of estimates produced. This has improved confidence in the results obtained, particularly at 10,000 years, as they are not significantly different from the estimated physical maximum limits of precipitable water at the site, i.e. PMP.

The climate change factors and projected precipitation amounts should be used with caution. There is still a large spread in the extreme precipitation amounts between the 11 models analysed here. Despite best efforts, this may still be due to a significant component of natural variability and in addition the spread may be due to the ensemble design to sample climate modelling uncertainty. The area over which the parameter containing the climate change signal has been averaged is arbitrary and is based on expert judgement of the spatial scale of the climate change signal.

The rainfall observations used come from a comparatively long period (roughly 100 years). However, it is possible that, by chance, the observations do not contain a representative sample of extreme events. There are no techniques currently available that allow an assessment of how representative a small period of data are of the “true” precipitation climatology without having access to that climatology.

The climate projections analysed in this report assume that there will not be any major volcanic activity during the 21st century (comparable to the eruption of Mt Pinatubo), and no major change in or collapse of the thermohaline circulation. These events would lead to major disruption to the UK climate. The climate projections have been generated with a single climate model. Other models may simulate different responses of UK precipitation to climate change. Similarly, climate projections using just one future emissions scenario have been analysed.

Only 11 regional climate model simulations were produced for UKCP09. Future work at the Met Office will attempt to use the UKCP09 methodology to produce probability distributions of changes in extreme weather utilising a statistical emulator to sample all the relevant uncertainties as discussed in section 4.2. These new data will allow a much improved estimation of the “true” distribution of precipitation extremes to be obtained thereby allowing a refining of the values derived in this study and providing a more robust level of confidence.

8. References

Bayliss, A. 1999. *Flood Estimation Handbook-5: Catchment Descriptors*, Institute of Hydrology, Wallingford.

Brown, S.J., J. Caesar, and C.A.T. Ferro, 2008. Global changes in extreme daily temperature since 1950. *J. Geophys. Res.*, 113, D05115, doi:10.1029/2006JD008091.

Buonomo E., R. Jones, C. Huntingford and J. Hannaford, 2007. On the robustness of changes in extreme precipitation over Europe from two high resolution climate change simulations, *Q. J. R. Meteorol. Soc.*, 133, 65-81, doi:10.1002/qj.13.

Clark C. 1995. New estimates of probable maximum precipitation in South West England. *Meteorological Applications*, Vol 2, p307-312.

Clark C. 1997. How rare is that storm in south-west England? *Meteorological Applications*, Vol 5, p139-148.

Coles, S., 2001. *An Introduction to modelling of extreme values*, Springer, London.

Collins, M., B.B.B. Booth, G.R. Harris, J.M. Murphy, D.M.H. Sexton, and M.J. Webb, 2006. Towards quantifying uncertainty in transient climate change, *Clim. Dyn.* 27, 127-147, doi:10.1007/s00382-006-0121-0.

Faulkner, D., 1999. *Flood Estimation Handbook-2: Rainfall Frequency Estimation*, Institute of Hydrology, Wallingford.

Glasspoole, J., 1924. The unprecedented rainfall at Cannington, August 18th, 1924. *British Rainfall*, pp.246-255, Edward Stanford, London.

Gordon, C., C. Cooper, C.A. Senior, H. Banks, J.M. Gregory, T.C. Johns, J.F.B. Mitchell and R.A. Wood, 2000. The simulation of SST, sea ice extents and ocean heat transports in a version of the Hadley Centre coupled model without flux adjustments, *Clim. Dyn.*, 16, 147-168.

Houghton-Carr, H. 1999. *Flood Estimation Handbook-4: Restatement and Application of the Flood Studies Report Rainfall-runoff Method*, Institute of Hydrology, Wallingford.

IPCC, 2000. Special Report on Emissions Scenarios. A special report of Working Group III of the Intergovernmental Panel on Climate Change, N. Nakićenović and R. Swart (eds). Cambridge University Press, Cambridge, UK. Available from: www.ipcc.ch

Jenkins, G.J., M.C. Perry, and M.J. Prior, 2008. *The climate of the United Kingdom and recent trends*, Met Office Hadley Centre, Exeter, UK.

Kharin, V.V. and F.W. Zwiers, 2005. Estimating extremes in transient climate simulations, *J. Climate*, 18, 1156-1173.

Kjeldsen, T., Jones, D., Bayliss, A., Spencer, P., Surendran, S., Stefan, L., Webster, P., McDonald, D. 2008 Improving the FEH statistical method. In: *Flood & Coastal Management Conference 2008, University of Manchester, 1-3 July 2008*. Environment Agency/Defra.

Lambert, F. H. and M. J. Webb, 2008: Dependency of global mean precipitation on surface temperature, *Geophys. Res. Lett.*, 35, L16706.

Lambert, F. H., A. R. Stine, N. Y. Krakauer and J. C. H. Chiang, 2008. How much will precipitation increase with global warming?, *EOS trans.*, 89, No. 21, doi: 10.1029/2008EO210001.

Lenderick, G and Van Meijgaard, E, 2008. Increase in hourly precipitation extremes beyond expectations from temperature changes, *Nature Geoscience*, 1, 511-514.

Lewis, 1991: *Meteorological Glossary*. Meteorological Office, London.

MacDonald, D. and Scott, C. 2000. *Revised design storm rainfall estimates obtained from the Flood Estimation Handbook (FEH)* in Dams 2000, Ed. P Tedd. Thomas Telford, London.

Murphy, J.M., D.M.H. Sexton, G.J. Jenkins, B.B.B. Booth, C.C. Brown, R.T. Clark, M. Collins, G.R. Harris, E.J. Kendon, R.A. Betts, S.J. Brown, K.A. Humphrey, M.P. McCarthy, R.E. McDonald, A. Stephens. C. Wallace, R. Warren, R. Wilby and R.A. Wood, 2009. *UK Climate Projections Science Report: Climate Change Projections*. Met Office Hadley Centre, Exeter, UK.

NERC, 1975. *Flood Studies Report*, Vol II, Meteorological Studies. Natural Environment Research Council, UK.

Perry M.C., and Hollis D.M., 2005. The generation of monthly gridded datasets for a range of climatic variables over the UK. *International Journal of Climatology* 25. pp. 1041-1054.

Reed, D. 1999. *Flood Estimation Handbook-1*: Overview, Institute of Hydrology, Wallingford.

Robson, A. and Reed, D. 1999. *Flood Estimation Handbook-3: Statistical procedures for flood frequency estimation*, Institute of Hydrology, Wallingford.

Stewart, E. J., Jones, D. A., Svensson, C., Morris, D. G., Dempsey, P., Dent, J. E., Collier, C. G. and Anderson, C. A. 2010. *Reservoir Safety - Long Return Period Rainfall.* Wallingford, Centre for Ecology and Hydrology. (CEH Project Number: C02760)

US Corps of Engineers, 1997. *Hydrologic Engineering Requirements for Reservoirs*. Engineer Manual 1110-2-1420, Washington D C.

WMO, 1986. *Manual for estimation of probable maximum precipitation*. Second edition. Operational Hydrology Report No. 1. WMO No. 332. World Meteorological Organisation (WMO), Geneva, Switzerland.

WMO, 1994. *Guide to Hydrological Practices*, WMO no. 168, 5th Edition. World Meteorological Organisation (WMO), Geneva, Switzerland.

WMO, 2009. *Guide to Hydrological Practices*, WMO no. 168, 6th Edition. World Meteorological Organisation (WMO), Geneva, Switzerland.

9. Appendix

9.1 Flood Estimation Handbook

The Flood Estimation Handbook (FEH) and accompanying software (FEH-CDROM) is the result of a concerted research effort by the Centre of Ecology and Hydrology (CEH) and its predecessor the Institute of Hydrology (IoH) and generally replaces the 1975 Flood Studies Report (FSR) (NERC, 1975). Some aspects of the FSR findings, e.g. design storm profiles and depth/area and depth/duration relationships are retained by FEH. The FEH aims to offer a consistent and clear solution to rainfall and flood frequency estimation for the analysis of historic events and, more critically, the design of structures influenced by river flow. The standard approach uses the methods and data incorporated in the FEH CD-ROM. By selection of appropriate data requirements estimates of rainfall depths for any duration and return period for any location or catchment in the UK can be obtained.

The FEH CD-ROM (Ver. 2.0) has been utilised in this section of the study to provide rainfall depths at Hinkley Point. The methodology implicit in the FEH-CDROM obtains rainfall estimates based on the 'pooling' of representative local rain gauge records stored within the FEH within a radius from a specified point of interest. The stored records consist of AMAX (annual maxima) rainfalls of varying lengths and for durations of 1 hour to 8 days from over 6000 rain gauges in the UK. A depth-duration-frequency (DDF) model has been constructed from these data within the FEH and can confidently be applied to obtain rainfall estimates for storm durations of between 1 hour and 8 days out to a return period of 1,000 years. Any estimates beyond these confines (e.g. 15-minute rainfall durations and 10,000 year return periods) are produced by extrapolating the model and should therefore be treated with caution. Therefore the FEH results should not be applied in isolation, and analysis of local gauge records should be conducted as a method of checking. For more information regarding the underlying data sources and methodologies within the FEH, Volumes I-V of the FEH (Bayliss, 1999, Faulkner, 1999, Houghton-Carr, 1999, Reed, 1999 and Robson and Reed, 1999,) should be consulted.

9.2 Summary of rain gauge record data

Year	Months Missing
1978	Aug, Sept, Oct
1981	Aug, Nov, Dec
1982	Aug
1983	Aug-Dec
1984-1995	Jan-Dec

Table 21. Summary of missing data in the digitised record at Cannington Farm Institute

Year	Months Missing
1959-1961	Jan-Dec
1996	Mar-Dec
1997-1998	Jan-Dec
1999	Jan-Jun
2006	Aug, Sept, Oct
2007	Mar
2009	Nov, Dec

Table 22. Summary of missing data in the digitised record at Brymore School

Year	Months Missing
1979	Aug
1984	Feb
1985	Dec
1987	Oct
1988	Aug
1999	Aug
2001	May
2002	Jan, Jul, Aug, Sept, Oct, Nov, Dec
2003	Apr, May, Jun-Dec
2004	May, Jun, Aug-Dec
2005	Jan-Dec

Table 23. Summary of missing data in the digitised record at Whitewick Farm

9.3 Maximum likelihood estimation

Maximum likelihood estimation (MLE) is a statistical method used for fitting a statistical model to data, and providing estimates for the model's parameters. If the model parameters are known, the probability of a given event occurring may be calculated. MLE turns this concept around, and allows the likelihood of these parameters being correct to be calculated, given the data.

A simple example of MLE may be illustrated by flipping a coin. The coin will always land heads or tails, and if it is unbiased, the probability of the coin landing either heads or tails will be 0.5.

The probability of obtaining a particular number of heads and tails can be calculated using the binomial probability distribution equation, which is:

Equation 17

$$P = \frac{n!}{h!(n-h)!} p^h (1-p)^{n-h}$$

where P is the probability of a particular number of heads and tails occurring, n is the total number of times the coin is flipped, h is the number of heads obtained, and p is the probability of obtaining a heads. If the probability of obtaining a head is 0.5, then the probability of obtaining a given number of heads (= P) may be easily found from the equation.

However, instead of assuming the probability of obtaining a heads is 0.5, this probability can be estimated using MLE. Suppose the coin was flipped 100 times, and 52 heads and 48 tails were obtained (so n = 100 and h = 52). Many values of p may be used in the equation, from which corresponding values of P are obtained. Now, P is the likelihood, and the value of p which gives the greatest value of P (the maximum likelihood) is the best estimate of the value of p. The MLE value is thus the largest likelihood value, and in this simple example will be 0.52. In practice, MLE is much more complex, as the model which will be fitted to the data will have more than one unknown parameter.

9.4 100 year precipitation tables accounting for climate change

2010-2039: Winter				
%ile	Change Factor	15 minute	1 hour	1 day
5th	1.00	33.3	44.7	92.8
25th	1.05	33.9	45.6	97.1
50th	1.07	34.1	46.1	99.1
68th	1.08	34.3	46.4	100.4
75th	1.09	34.4	46.5	100.9
84th	1.10	34.5	46.7	101.7
95th	1.12	34.7	47.1	103.3

2010-2039:Summer				
%ile	Change Factor	15 minute	1 hour	1 day
5th	0.90	32.1	42.4	83.2
25th	0.99	33.2	44.4	91.9
50th	1.02	33.5	44.9	94.1
68th	1.05	33.9	45.6	97.0
75th	1.06	34.0	45.8	97.8
84th	1.06	34.1	46.0	98.6
95th	1.08	34.2	46.3	99.9

2020-2049: Winter				
%ile	Change Factor	15 minute	1 hour	1 day
5th	1.00	33.3	44.7	92.9
25th	1.06	34.0	45.9	98.4
50th	1.09	34.4	46.6	101.1
68th	1.11	34.6	46.9	102.7
75th	1.12	34.7	47.1	103.4
84th	1.13	34.8	47.3	104.4
95th	1.15	35.1	47.8	106.4

2020-2049:Summer				
%ile	Change Factor	15 minute	1 hour	1 day
5th	0.87	31.8	41.8	80.7
25th	0.99	33.2	44.4	91.7
50th	1.02	33.5	45.0	94.5
68th	1.06	34.0	45.9	98.4
75th	1.07	34.2	46.2	99.4
84th	1.08	34.3	46.4	100.4
95th	1.10	34.5	46.8	102.1

2030-2059: Winter				
%ile	Change Factor	15 minute	1 hour	1 day
5th	1.00	33.3	44.7	93.0
25th	1.08	34.2	46.3	99.7
50th	1.11	34.7	47.0	103.1
68th	1.14	34.9	47.5	105.1
75th	1.14	35.0	47.7	105.9
84th	1.16	35.2	48.0	107.2
95th	1.18	35.5	48.6	109.7

2030-2059:Summer				
%ile	Change Factor	15 minute	1 hour	1 day
5th	0.84	31.4	41.3	78.2
25th	0.99	33.2	44.3	91.5
50th	1.03	33.6	45.2	95.0
68th	1.08	34.2	46.3	99.8
75th	1.09	34.4	46.6	101.0
84th	1.10	34.6	46.8	102.3
95th	1.13	34.8	47.3	104.4

2040-2069: Winter				
%ile	Change Factor	15 minute	1 hour	1 day
5th	1.01	33.4	44.7	93.1
25th	1.09	34.4	46.6	101.1
50th	1.14	34.9	47.5	105.2
68th	1.16	35.2	48.1	107.6
75th	1.17	35.4	48.3	108.6
84th	1.19	35.6	48.7	110.1
95th	1.22	36.0	49.4	113.2

2040-2069:Summer				
%ile	Change Factor	15 minute	1 hour	1 day
5th	0.82	31.1	40.7	75.7
25th	0.99	33.1	44.3	91.2
50th	1.03	33.7	45.3	95.4
68th	1.09	34.4	46.6	101.3
75th	1.11	34.6	46.9	102.7
84th	1.13	34.8	47.3	104.3
95th	1.15	35.1	47.9	106.8

Table 24. 1 in 100 year rainfall estimates (in mm) for durations of 15 minutes, 1 hour and 1 day at Hinkley Point by season for 2010-2039, 2020-2049, 2030-2059 and 2040-2069 (A1B Scenario) for a range of percentiles.

2050-2079: Winter				
%ile	Change Factor	15 minute	1 hour	1 day
5th	1.01	33.4	44.7	93.2
25th	1.11	34.6	46.9	102.4
50th	1.16	35.2	48.0	107.1
68th	1.19	35.5	48.6	109.9
75th	1.20	35.7	48.9	111.1
84th	1.22	35.9	49.3	112.9
95th	1.26	36.4	50.1	116.5

2050-2079:Summer				
%ile	Change Factor	15 minute	1 hour	1 day
5th	0.79	30.8	40.2	73.6
25th	0.98	33.1	44.2	91.0
50th	1.04	33.7	45.4	95.9
68th	1.11	34.6	46.9	102.6
75th	1.13	34.8	47.3	104.3
84th	1.15	35.0	47.7	106.1
95th	1.18	35.4	48.4	109.1

2060-2089: Winter				
%ile	Change Factor	15 minute	1 hour	1 day
5th	1.01	33.4	44.8	93.3
25th	1.12	34.7	47.2	103.6
50th	1.18	35.4	48.4	109.0
68th	1.21	35.8	49.2	112.2
75th	1.23	36.0	49.5	113.6
84th	1.25	36.3	49.9	115.6
95th	1.29	36.8	50.9	119.8

2060-2089:Summer				
%ile	Change Factor	15 minute	1 hour	1 day
5th	0.77	30.6	39.7	71.5
25th	0.98	33.1	44.2	90.9
50th	1.04	33.8	45.5	96.3
68th	1.12	34.8	47.2	103.9
75th	1.14	35.0	47.7	105.9
84th	1.17	35.3	48.2	107.9
95th	1.20	35.7	49.0	111.5

2070-2099: Winter				
%ile	Change Factor	15 minute	1 hour	1 day
5th	1.01	33.4	44.8	93.3
25th	1.13	34.9	47.4	104.7
50th	1.19	35.6	48.8	110.6
68th	1.23	36.1	49.6	114.2
75th	1.25	36.3	50.0	115.7
84th	1.27	36.6	50.5	118.0
95th	1.33	37.2	51.6	122.7

2070-2099:Summer				
%ile	Change Factor	15 minute	1 hour	1 day
5th	0.75	30.4	39.3	69.8
25th	0.98	33.1	44.2	90.7
50th	1.04	33.8	45.5	96.7
68th	1.13	34.9	47.5	105.0
75th	1.16	35.2	48.0	107.2
84th	1.18	35.5	48.5	109.5
95th	1.23	36.0	49.5	113.5

Table 24. (continued) 1 in 100 year rainfall estimates (in mm) for durations of 15 minutes, 1 hour and 1 day at Hinkley Point by season for 2050-2079, 2060-2089 and 2070-2099 (A1B Scenario) for a range of percentiles.

Duration	Winter	Summer
	Range of estimates (mm)	Range of estimates (mm)
15 minutes	33.3-37.2	30.4-36.0
1 hour	44.7-51.6	39.3-49.5
1 day	92.8-122.7	69.8-113.5

Table 25. Range of 100 year rainfall estimates accounting for climate change to 2099.

9.5 1,000 year precipitation tables accounting for climate change

2010-2039: Winter				
%ile	Change Factor	15 minute	1 hour	1 day
5th	1.00	69.4	85.3	145.0
25th	1.05	71.0	87.8	152.3
50th	1.07	71.8	89.0	155.9
68th	1.09	72.3	89.8	158.0
75th	1.09	72.5	90.1	158.9
84th	1.10	72.8	90.5	160.2
95th	1.12	73.4	91.4	162.8

2010-2039:Summer				
%ile	Change Factor	15 minute	1 hour	1 day
5th	0.89	65.9	80.0	129.7
25th	0.99	69.3	85.1	144.6
50th	1.02	70.1	86.4	148.2
68th	1.05	71.2	88.1	153.1
75th	1.06	71.5	88.6	154.5
84th	1.07	71.8	89.1	155.9
95th	1.09	72.4	89.9	158.3

2020-2049: Winter				
%ile	Change Factor	15 minute	1 hour	1 day
5th	0.99	69.3	85.2	144.8
25th	1.06	71.5	88.5	154.3
50th	1.09	72.5	90.1	159.0
68th	1.11	73.2	91.1	161.8
75th	1.12	73.4	91.5	162.9
84th	1.13	73.8	92.0	164.6
95th	1.15	74.6	93.2	168.0

2020-2049:Summer				
%ile	Change Factor	15 minute	1 hour	1 day
5th	0.86	64.9	78.5	125.4
25th	0.99	69.2	85.0	144.3
50th	1.02	70.3	86.7	149.0
68th	1.07	71.7	88.9	155.4
75th	1.08	72.1	89.5	157.2
84th	1.09	72.6	90.1	159.0
95th	1.11	73.3	91.2	162.1

2030-2059: Winter				
%ile	Change Factor	15 minute	1 hour	1 day
5th	0.99	69.3	85.2	144.6
25th	1.07	71.9	89.2	156.3
50th	1.11	73.3	91.2	162.2
68th	1.14	74.1	92.4	165.6
75th	1.15	74.4	92.9	167.0
84th	1.16	74.9	93.6	169.1
95th	1.19	75.8	95.1	173.4

2030-2059:Summer				
%ile	Change Factor	15 minute	1 hour	1 day
5th	0.83	63.9	77.1	121.2
25th	0.99	69.1	84.9	144.0
50th	1.03	70.5	87.0	149.8
68th	1.08	72.3	89.7	157.8
75th	1.10	72.8	90.5	160.0
84th	1.11	73.3	91.2	162.3
95th	1.14	74.2	92.6	166.1

2040-2069: Winter				
%ile	Change Factor	15 minute	1 hour	1 day
5th	0.99	69.2	85.1	144.5
25th	1.09	72.4	89.9	158.4
50th	1.14	74.0	92.4	165.5
68th	1.17	75.0	93.8	169.7
75th	1.18	75.4	94.4	171.3
84th	1.19	75.9	95.2	173.9
95th	1.23	77.1	97.0	179.0

2040-2069:Summer				
%ile	Change Factor	15 minute	1 hour	1 day
5th	0.80	63.0	75.7	117.1
25th	0.99	69.1	84.8	143.7
50th	1.03	70.6	87.2	150.6
68th	1.10	72.9	90.6	160.3
75th	1.12	73.4	91.5	162.9
84th	1.14	74.1	92.4	165.6
95th	1.17	75.1	94.0	170.3

Table 26. 1 in 1,000 year rainfall estimates (in mm) for durations of 15 minutes, 1 hour and 1 day at Hinkley Point by season for 2010-2039, 2020-2049, 2030-2059 and 2040-2069 (A1B Scenario) for a range of percentiles.

2050-2079: Winter				
%ile	Change Factor	15 minute	1 hour	1 day
5th	0.99	69.2	85.1	144.4
25th	1.10	72.8	90.6	160.3
50th	1.16	74.7	93.4	168.6
68th	1.19	75.8	95.1	173.5
75th	1.20	76.3	95.8	175.4
84th	1.23	77.0	96.8	178.4
95th	1.27	78.4	98.9	184.5

2050-2079:Summer				
%ile	Change Factor	15 minute	1 hour	1 day
5th	0.78	62.2	74.4	113.5
25th	0.98	69.0	84.7	143.4
50th	1.04	70.8	87.5	151.4
68th	1.12	73.4	91.4	162.6
75th	1.14	74.1	92.4	165.6
84th	1.16	74.8	93.5	168.8
95th	1.20	76.1	95.4	174.4

2060-2089: Winter				
%ile	Change Factor	15 minute	1 hour	1 day
5th	0.99	69.2	85.0	144.3
25th	1.11	73.3	91.2	162.1
50th	1.18	75.4	94.5	171.6
68th	1.22	76.7	96.4	177.2
75th	1.23	77.2	97.2	179.4
84th	1.26	78.0	98.3	182.9
95th	1.30	79.6	100.8	190.0

2060-2089:Summer				
%ile	Change Factor	15 minute	1 hour	1 day
5th	0.76	61.4	73.2	110.1
25th	0.98	68.9	84.7	143.1
50th	1.05	71.0	87.8	152.2
68th	1.13	73.9	92.1	164.8
75th	1.16	74.7	93.3	168.3
84th	1.18	75.5	94.6	172.0
95th	1.23	77.0	96.8	178.4

2070-2099: Winter				
%ile	Change Factor	15 minute	1 hour	1 day
5th	0.99	69.2	85.0	144.2
25th	1.12	73.6	91.8	163.8
50th	1.20	76.0	95.4	174.2
68th	1.24	77.4	97.5	180.4
75th	1.26	78.0	98.4	183.0
84th	1.28	78.9	99.7	186.8
95th	1.34	80.7	102.5	194.8

2070-2099:Summer				
%ile	Change Factor	15 minute	1 hour	1 day
5th	0.74	60.7	72.3	107.2
25th	0.98	68.9	84.6	142.9
50th	1.05	71.1	88.0	152.8
68th	1.15	74.3	92.8	166.7
75th	1.17	75.2	94.1	170.6
84th	1.20	76.1	95.6	174.7
95th	1.25	77.8	98.0	182.0

Table 26 (continued) 1 in 1,000 year rainfall estimates (in mm) for durations of 15 minutes, 1 hour and 1 day at Hinkley Point by season for 2050-2079, 2060-2089 and 2070-2099 (A1B Scenario) for a range of percentiles.

Duration	Winter	Summer
	Range of estimates (mm)	Range of estimates (mm)
15 minutes	69.2-80.7	60.7-77.8
1 hour	85.0-102.5	72.3-98.0
1 day	144.2-194.8	107.2-182.0

Table 27. Range of 1,000 year rainfall estimates accounting for climate change to 2099.

Met Office
FitzRoy Road, Exeter
Devon EX1 3PB
United Kingdom

Tel: 0870 900 0100
Fax: 0870 900 5050
enquiries@metoffice.gov.uk
www.metoffice.gov.uk